Atomistic insights into the partial oxidation of methanol using gold single crystal surfaces

Inaugural-Dissertation

to obtain the academic degree

Doctor rerum naturalium

(Dr. rer nat.)

submitted to the Department of Biology, Chemistry, Pharmacy

of Freie Universität Berlin

by

Salma Eltayeb

from Sudan

Berlin, 2024

This dissertation has been prepared between June 2021 and May 2024 in the group of Prof. Dr. Thomas Risse in the department of Physical and Theoretical Chemistry, Freie Universität Berlin, Arnimallee 22, 14195 Berlin.

First reviewer: Prof. Dr. Thomas Risse
Second reviewer: Prof. Dr. Christian Papp
Date of defense: 09.12.2024

"*I got my start by giving myself a start*."

Madam C. J. Walker

Acknowledgments

I still recall the day when I sent an email to Prof. Dr. Thomas Risse expressing my keen interest in catalysis and my desire to join his research group. Little did I know that this simple email would mark the beginning of an extraordinary academic journey, filled with challenges, discoveries, and immense personal growth. First, I want to thank Prof. Dr. Thomas Risse for his exceptional mentorship and unwavering support throughout my doctoral studies. His expertise and guidance have been invaluable in shaping my research and academic growth. My gratitude goes to Prof. Dr. Christian Papp for being the second referee for my thesis.

I extend my sincere gratitude to Dr. Wiebke Riedel, who has been a remarkable monitor and supervisor in the lab. Her meticulous supervision and invaluable support in proofreading my thesis have been crucial in ensuring the rigor and clarity of my work.

Dr. Christoph Feldt had introduced me into the experimental handling, I am grateful for his extraordinary helpfulness and many fruitful discussions about the concerning physics behind the experiments. Our former technician Rudolf Cames for technical support. I thank my students, Yiran Zhang, Henrik Wiedenhaupt, Lukas Dippel, Valentin Stefan Runz and Benjamin Switon who did a great job during their internships and bachelor theses. Furthermore, I thank my current and former colleagues John Michael Correa and Keyun Tang for their technical support.

My special thank goes to Hendrik Ronneburg who helped me out with various technical issues and scientific questions, and Weronika Malicka, Zohreh Asadi and Tamasri Senapati for the delightful early morning coffee breaks and spontaneous meetings we shared. Of course, I also want to thank all other current and former members of the AG Risse, Dr. Marina Pigaleva, Polina Ponomareva and Tomislav Kremer.

I thank our theoretical collaborator Prof. Lyudmila Moskaleva for her time and effort in addressing complex scientific questions from a computational prospective. Her insights have played an important role in enhancing the understanding of our experimental investigations.

Additionally, I thank Elsa-Neumann-Stiftung, Ernst-Reuter-Gesellschaft and the Ministry of Higher Education in Sudan, for their generous financial support. Without your funding, this research endeavor would not have been possible. Lastly, I dedicate this thesis to my family, for their unwavering encouragement and support.

Declaration of Independence

Herewith I certify that I have prepared and written my thesis independently and that I have not used any sources and aids other than those indicated by me.

Berlin, 12.09.2024 *Salma Eltayeb*

Abstract

The partial oxidation of methanol to methyl formate (MeFo) proceeds with high selectivity at high conversion on nanoporous gold (np-Au) catalysts. To obtain fundamental insights into the surface processes required for a rational improvement of this catalyst, a surface science approach investigating simplified model catalysts under well-defined single-collision conditions is used. Pulsed molecular beam (MB) experiments allow to study the transient and steady state kinetics under isothermal conditions and thereby for comparison to the applied systems. As np-Au catalysts contain, next to terraces, a high number of low-coordinated surface sites (LCS), the reactivity of flat Au(111) was compared to stepped Au(332) exhibiting (111)-terraces separated by monoatomic steps and thus, a notable number of LCS. These LCS enhance at high temperatures MeFo formation and lower overoxidation, as desired for an ideal partial oxidation catalyst. For low coverage conditions preferential adsorption of reactants at LCS enhances the selectivity for the coupling product, whereas conditions with higher surface coverage, e.g. at low temperatures, lower the MeFo selectivity, as adsorbates can act as obstacles for successful reactant encounters required for the coupling reaction. In addition to LCS, accumulated Au_xO_y-phases play a crucial role for understanding the observed chemistry. If formed at step sites density functional theory calculations from our collaborators reveal increased barriers for unwanted overoxidation explaining the experimentally observed differences in selectivity. Moreover, MeFo formation may require or benefit from Au_xO_y-phases, especially at step sites, as indicated by the experimental transient kinetics. As water is an oxidation product and a common (methanol) feed impurity, it may affect under applied multi collision conditions the methanol oxidation on np-Au catalysts. MB experiments on model catalysts conducted with and without added water demonstrated that in case of oxygen rich conditions water has a detrimental effect on MeFo formation rationalized by hydrogen-bonding with methanol as well as by reaction with adsorbed oxygen e.g. affecting the formation of Au_xO_y-phases and thus their beneficial effect at steps in suppressing overoxidation. Yet, under oxygen-poor, low coverage conditions, the negative effect of water decreases and almost disappears for Au(332) exhibiting a high number of LCS. This allows to propose a rationale for diverse findings for the impact of water on methanol oxidation in liquid and gas phases on np-Au, as these results provide insights into conditions critical for high selectivity in partial oxidation.

Zusammenfassung

Die partielle Oxidation von Methanol zu Methylformiat (MeFo) verläuft mit hoher Selektivität bei hohem Umsatz auf nanoporösen Gold-Katalysatoren (np-Au). Um grundlegende Einblicke in die Oberflächenprozesse zu erhalten, welche notwendig für die rationale Verbesserung dieses vielversprechenden Katalysators sind, werden vereinfachte Modellkatalysatoren unter wohl-definierten Bedingungen untersucht. Experimente mit gepulsten Molekularstrahlen (engl. molecular beam, MB) erlauben es, die transiente und quasi-stationäre Kinetik unter isothermen und Einzelstoß-Bedingungen zu untersuchen und mit katalytischen Eigenschaften der angewandten Systeme zu vergleichen.

Da np-Au neben Terrassen auch eine hohe Anzahl von niedrig-koordinierten Oberflächenplätzen (engl. low-coordinated sites, LCS) aufweist, wurde die Reaktivität von flachen Au(111)- mit der von gestuftem Au(332)-Oberflächen verglichen. Letztere hat neben (111)-Terrassen auch regulär angeordnete, monoatomare Stufen, so dass die Oberfläche eine signifikante Anzahl an LCS aufweist. Die LCS erhöhen bei hohen Temperaturen die Methylformiat-Bildung und erniedrigen ungewollte Überoxidation, so wie es für einen idealen Partialoxidationskatalysator gewünscht ist. Für niedrige Bedeckungen erhöht die bevorzugte Adsorption von Reaktanden an LCS die Selektivität zum Kopplungsprodukt, wohingegen sie bei höheren Bedeckungen, wie z.B. bei niedrigen Temperaturen, die MeFo-Selektivität erniedrigen, da Adsorbate auch Hindernisse für erfolgreiche Begegnungen der Reaktanden darstellen können, welche für die Kopplungsreaktion benötigt werden. Zusätzlich zu LCS spielen akkumulierte Au_xO_y-Phasen eine wichtige Rolle für das Verständnis der beobachteten Chemie. Für solche, die an Stufenplätzen gebildet werden, zeigen Dichte-Funktional-Rechnungen unserer Kooperationspartner erhöhte Barrieren für ungewollte Überoxidation, was die experimentell beobachteten Selektivitätsunterschiede erklärt. Es konnte gezeigt werden, dass akkumulierte Au_xO_y-Phasen wenn nicht essentiell so zumindest förderlich für die MeFo Bildung sind, wobei aufgrund der transienten Kinetik insbesondere den Spezies an Stufenplätzen eine wichtige Rolle zukommt.

Da Wasser ein Oxidationsprodukt und eine häufige Verunreinigung des (Methanol-) Ausgangsmaterials ist, kann es unter den Bedingungen der Methanol-Oxidation auf np-Au die Eigenschaften der Katalysatoren merklich beeinflussen. MB-Experimente auf

Modellkatalysatoren, die mit und ohne hinzugefügtes Wasser durchgeführt wurden, haben gezeigt, dass Wasser unter sauerstoffreichen Bedingungen einen nachteiligen Effekt auf die MeFo-Bildung hat. Dies kann zum einen auf die Bildung von Wasserstoff-Brücken zu Methanol und zum anderen auch auf Reaktionen mit adsorbiertem Sauerstoff zurückgeführt werden, wobei Letztere z.B. die Bildung von Au_xO_y-Phasen beeinflussen und so deren vorteilhaften Effekt an Stufen auf die ungewollte Überoxidation aufheben. Unter sauerstoffarmen Bedingungen und niedrigen Bedeckungen wird der negative Effekt von Wasser kleiner und verschwindet für die Au(332)-Oberfläche mit einer signifikanten Anzahl an LCS fast ganz. Diese Beobachtung erlaubt es die sehr unterschiedlichen Beobachtungen zur Wirkung von Wasser auf die Methanol-Oxidation auf np-Au in flüssiger Phase und in der Gasphase zu verstehen, da die Ergebnisse Einblicke in die Bedingungen geben, die notwendig sind, um hohe Selektivität für partielle Oxidationsprodukte auf np-Au-Katalysatoren zu erzielen.

The translation into German was done by Dr. Wiebke Riedel.

List of Publications

Paper I

Partial oxidation of methanol on gold: How selectivity is steered by low-coordinated sites

Salma Eltayeb, Lenard L. Carroll, Lukas Dippel, Mersad Mostaghimi, Wiebke Riedel, Lyudmila Moskaleva and Thomas Risse, ACS catalysis **2024**, 14, 10, 7901–7906.

DOI: https://doi.org/10.1021/acscatal.3c04578

Paper II

Selective oxidation of methanol to methyl formate on gold: The role of low-coordinated sites revealed by isothermal pulsed molecular beam experiments and AIMD simulations

Salma Eltayeb, Lenard L. Carroll, Lukas Dippel, Mersad Mostaghimi, Wiebke Riedel, Lyudmila Moskaleva and Thomas Risse, The Journal of Physical Chemistry C **2024**.

DOI: https://doi.org/10.1021/acs.jpcc.4c03959

Paper III

Unraveling the role of water in isothermal methanol partial oxidation to methyl formate on gold: A combined experimental and computational study

Salma Eltayeb, Lenard L. Carroll, John Michael Correa Hoyos, Christoph D. Feldt, Benjamin Switon, Wiebke Riedel, Lyudmila Moskaleva and Thomas Risse, submitted to The Journal of Physical Chemistry C **2024**. DOI: https://doi.org/10.1021/acs.jpcc.4c05968

Contents

1 Introduction

Catalysis, a fundamental concept in chemistry, refers to the process by which the rate of a chemical reaction is increased through the introduction of a catalyst, which participate in the reaction, but ideally are chemically unchanged at the end of the catalytic cycle. This process is integral to numerous industrial applications, ranging from the production of fuels and pharmaceuticals to environmental protection and energy generation, as it enables reactions to proceed under milder conditions, improves reaction selectivity, and enhances yield, thereby making processes more efficient and economically viable.[1, 2] Heterogeneous catalysts, often solid catalysts interacting with reactants in gas or liquid phase, are widely used in industrial applications due to the ease of separation of the catalyst from the reaction mixture and its reusability. Typically, reactants adsorb on the surface of solid catalysts forming intermediates at active sites facilitating thereby through a number of steps the formation of products. The surface of an industrially used solid catalyst is not uniform. On the one hand, most catalysts consist of different chemical elements influencing the reactivity of the catalyst. On the other hand, even the surface of a pure metal typically exhibits a variety of sites, including terraces, edges, and corners, which vary in coordination number and electronic properties affecting their activity and selectivity.[3, 4]

Oxidation reactions, especially partial oxidations, are essential transformations in chemical industry.[5] However, the use of harsh oxidants is not only often detrimental to the selectivity, but also threatening the ecosystem and public health.[3] Therefore, catalysts enabling the use of widely available and environmentally friendly oxidants, such as molecular oxygen, are of particular interest in case they allow high conversion combined with high selectivity towards the desired product which is oftentimes not the thermodynamically most favored one. Hence, rendering the stable kinetic control of the reaction network crucial to achieve this goal.

Gold, traditionally considered an inert and unreactive metal, has emerged as a remarkable catalyst, especially in the field of low temperature oxidation reactions.[3, 6, 7] Au nanoparticles on oxide supports have demonstrated remarkable catalytic activity, as first reported by Haruta, catalyzing e.g. aerobic CO oxidation at low temperatures.[8, 9] The catalytic activity of these supported Au

nanoparticle catalysts requires very small particle sizes (< 5 nm) and the interaction with a metal oxide support plays an important role for the catalytic activity.[10, 11] Therefore, the development of active self-supported nanoporous gold (np-Au) catalysts, which feature significantly larger Au ligaments and lack a metal oxide support, marked a fascinating advancement in gold catalysis. The catalytic activity of this unsupported, fully metallic material was based on the findings for supported Au nanoparticle catalyst unexpected as it exhibits feature sizes about an order of magnitude larger than the nanoparticles and lacks an oxidic support. This discovery challenges the previously accepted notion that gold must be in the form of very small nanoparticles (a few nanometers) interacting with an oxide support to serve as an active oxidation catalyst.[7, 9, 12-17] Np-Au is created through a dealloying process, where a less noble metal, such as silver (Ag), is selectively leached out of an alloy containing gold, resulting in a porous structure with high surface area.[15, 18, 19] This porous structure is a highly effective catalyst in various reactions, including oxidation reactions and organic transformations already at low temperatures.[12, 20] Carbon monoxide (CO) oxidation over these catalysts was found at temperatures as low as − 30 °C.[19, 21] The interest in the system was boosted significantly after showing a high activity towards selective oxidative coupling reaction, including the oxidative coupling of methanol to methyl formate (MeFo). The formation of MeFo from partial oxidation of methanol over Au catalysts differs from the common product distributions seen with other metals favoring the formation of e.g. formaldehyde or carbon dioxide (CO_2).[22-24]

MeFo is an important industrial product being used for the production of more than 50 chemicals, including formic acid, N,N-dimethylformamide, formamide and dimethyl carbonate.[25] Industrially MeFo is produced mainly by carbonylation of methanol with a global production capacity of > 6 million tons in 2016.[26] The current industrial production route, however, requires water and CO_2 free reactant feeds which renders alternative routes, such as dehydrogenation or aerobic partial oxidation of methanol, promising approaches.[25] Thus, the high activity and selectivity of np-Au catalysts for the oxidative coupling of methanol to MeFo at low temperatures[13, 20], makes np-Au a promising catalyst for a green transformation of methanol using atmospheric oxygen.[27] A reaction mechanism for MeFo formation from the selective methanol oxidation was proposed based on model studies. The multistep reaction mechanism begins with the formation of methoxy through the abstraction of the acidic proton from methanol by activated oxygen, followed by β-H elimination step that generates formaldehyde. The formaldehyde then couples with another

methoxy to eventually form MeFo and by-product water.[28-30] The selectivity towards this partial oxidation product was reported to decrease for high oxygen concentrations and high amounts of residual Ag in the np-Au, whereas total oxidation is favored under these conditions.[20] This observation is consistent with the notion that small, residual amounts of Ag are crucial for the activation of molecular oxygen[31, 32], which is not possible on pure Au[33, 34] and is the rate limiting step in aerobic oxidations over Au catalysts.[20, 31, 35-37] Overoxidation is not only affected by the Ag content, but also the type of oxygen species on the Au surface, such as different oxidic phases,[38, 39] may favor overoxidation of methanol.[22] Yet, it should be emphasized that the average oxygen coverage on np-Au under typical reaction conditions is low (approx. 0.004 ML).[35, 40] Apart from high oxygen partial pressures, decreasing selectivity towards MeFo at the expense of total oxidation was reported for increasing temperatures, while methanol conversion was reported to increase.[41] Next to overoxidation, also formaldehyde formation may compete with MeFo formation, the former being favored by short contact times.[35] While some factors influencing selectivity and activity of the catalyst agrees with general expectations, such as high oxygen concentrations favoring overoxidation, the effect of others on the catalytic system cannot be unraveled from studies of np-Au catalysts. One aspect is the role of low-coordinated sites (LCS) for the catalytic properties, present in large proportions on np-Au catalysts.[18, 19] While these sites were previously suggested to influence catalytic activity and selectivity,[42, 43] experimental proof was scarce due to the complexity of isolating their impact on the catalytic properties for such a complex system. Moreover, under applied multiple-collision conditions in np-Au, the products as well as gas phase intermediates may re-adsorb on the surface and undergo subsequent reactions, before exiting the catalyst bed. Apart from intermediates also by-products of the reaction -for this particular reaction water- may affect the selectivity by altering the importance of different reaction channels. While a significant enhancement for CO oxidation yield in the presence of water was reported,[28, 44, 45] a dramatic decrease of MeFo selectivity in liquid phase methanol oxidation was found on np-Au in case the liquid contained water. The latter is surprising considering the high MeFo selectivities at high conversion in gas phase methanol oxidation on np-Au suggesting that water close to equimolar compositions in the gas phase does not significantly affect methanol oxidation on np-Au.[20, 46]

Gaining an atomic- and molecular-level understanding of the surface process, which is required for a rational improvement of these promising catalysts, is challenging for an applied complex

catalyst, such as np-Au. One strategy to address these questions is to investigate simplified model systems. In this respect, studies of well-defined model systems under ultra-high vacuum (UHV) conditions using the toolbox of modern surface science methodology have shown to be a powerful strategy to provide an atomic-level understanding of catalytic processes.[18, 47] With this approach, a number of aspects have been successfully addressed. Most of these model studies were carried out on low-index Au surfaces, such as Au(111)[12, 28, 48, 49] which do not contain a significant number of LCS as found in np-Au. For reactivity investigations, aside from recent studies under isothermal conditions[50, 51], mostly temperature programmed reaction (TPR) measurements have been used thus far where the reactants are adsorbed at low temperatures onto the surface and the desorbing products are monitored during a subsequent heating of the surface.[52] However, isothermal, pulsed molecular beam (MB) experiments offer significant advantages over traditional TPR studies by providing real-time insights into surface processes during catalytic reactions. These experiments allow for the precise control and monitoring of reactant pulses under constant temperature conditions, which can reveal transient behaviors and intermediate species that are often obscured in TPR studies. Recent studies on methanol oxidation on stepped gold surfaces under isothermal conditions have provided deeper insights into the catalytic mechanisms involved, as they reveal the dynamics of intermediate species, reaction pathways, and the role of surface defects in facilitating or hindering specific reactions.[50, 51] A more detailed representation of the results from model studies can be found in Chapter 2. Despite the effort that has been made, important questions remain open: Low-coordinated sites were proposed to critically influence the catalytic properties, however, direct (experimental) investigations of this are limited.[42, 43] Moreover, various oxygen species may be involved in the oxidation process, requiring further investigation to identify their reactivity, selectivity, and specific roles in the reaction pathway. In addition, the influence of the increasing concentrations of the by-product water, as found for high conversion of methanol to MeFo, has been only scarcely investigated by model studies,[50] despite the reported effects of water on oxidation of CO as well as of methanol over np-Au catalysts.[28, 44, 45] In this thesis, the oxidative coupling of methanol on gold surfaces was investigated under well-defined conditions employing Au single crystal surfaces as model systems to provide important new insights into these open questions required to understand the catalysis of np-Au.

The aim of this work

The central aim of this thesis, is to enhance the atomic level understanding of the (partial) oxidation of methanol on Au surfaces by employing a surface science approach. In specific, the role of low-coordinated sites is addressed by comparing the reactivity on flat Au(111) with that of stepped Au(332) exhibiting 6-atom-wide (111)-terraces separated by close-packed monoatomic steps. Chemically this question is closely related with the speciation and reactivity of activated oxygen species on the surface. Moreover, the effect of water, a product as well as common (methanol) feed impurity is investigated. To achieve these aims, the isothermal reactivity of the model catalysts was investigated under well-defined single collision conditions using pulsed molecular beam studies coupled with time-resolved mass spectrometry for detection of gas phase species, such as MeFo, and combining these with in-situ IRAS measurements for studying surface adsorbed species. As single crystal Au surfaces do not activate molecular oxygen under UHV conditions, an effusive oxygen atom source with well-defined flux-characteristics was added to the molecular beam apparatus to facilitate these studies. This setup allows to control the flux of the reactants as well as their temporal structure which provides access to both steady state and transient kinetics providing valuable insights into the microscopic details of the chemical reactions taking place on Au surface.

The present thesis is organized as follows:

In **Chapter 2**, the theoretical background of the most important aspects with respect to this work is presented. A brief overview over specific aspects of kinetic processes on surfaces and a description of the physical working principles of the experimental methods applied in this work are given. Moreover, results from literature concerning the methanol (partial) oxidation on gold surfaces which are relevant for the results obtained in this work are summarized. In **Chapter 3**, the experimental details are given. In particular, the molecular beam (MB) apparatus, that was used to acquire the data presented in the subsequent chapters, is presented and the experimental details of the MB measurements performed in this study are described. In **Chapter 4**, the publications are summarized, and the corresponding scientific results discussed also in light of theoretical calculations conducted in the group of Prof. Moskaleva. The conclusion and an outlook are given in **Chapter 5** and the list of publications in **Chapter 6**.

2 Theoretical background

In this chapter, the theoretical background of the most important aspects in this work will be discussed. In the first section (2.1), specific aspects of dynamic and kinetic processes on surfaces will be presented. The physical working principle of the experimental methods applied in this work will be described in (2.2) and (2.3) including effusive molecular beams and characterization techniques used for the gold surfaces, respectively. In the fourth section (2.4), results from relevant literature on methanol (partial) oxidation on gold surfaces will be discussed.

2.1 Dynamic and specific kinetic processes on surfaces

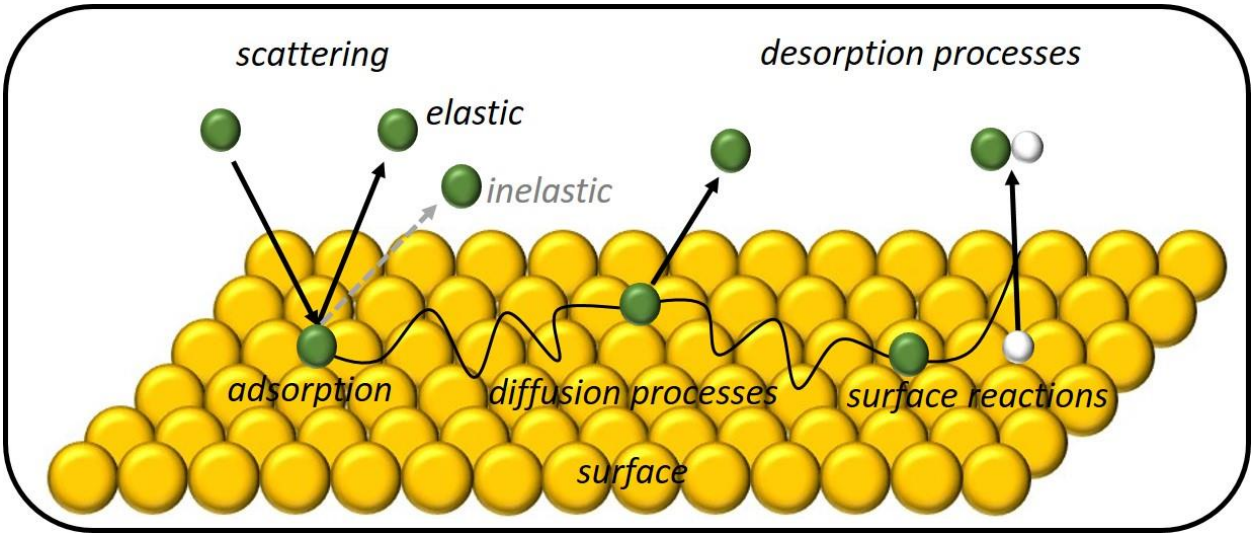

Figure 2.1: Schematic representation of basic processes in gas–surface interactions, adapted from ref.[53].

Understanding dynamic and kinetic processes on surfaces is essential in different fields, such as catalysis, material science, and surface chemistry, where controlling and manipulating interactions at the atomic or molecular level are crucial for designing functional materials and optimizing chemical processes. This understanding becomes particularly critical, when studying the kinetics of catalytic conversions of gases on a heterogeneous catalyst to obtain atomistic-level insights into the microscopic processes of the fundamental gas-surface interactions of the investigated system. A catalytic reaction at surfaces involves generally a sequence of several elementary reaction steps that might result in a complex kinetic behavior. Figure 2.1 illustrates the most important

elementary processes, which will be addressed in the following paragraphs. A more detailed discussion can also be found in the literature.[54-58]

2.1.1 Principles of adsorbate-surface interactions

Consider the fate of an atom or a molecule from the gas phase, which collides with the surface. After initial collision, the species may be elastically or inelastically scattered back into the gas phase. On the one hand, in an *elastic scattering* process, the particle is scattered without any energy exchange between the particle and the surface. Thus, the particle is reflected without any possibility to stick, and the energy of the particle and the surface is conserved. In an *inelastic scattering* event, on the other hand, energy is transferred between the impinging particle and the surface involving phonon or electronic processes. The particle may transfer energy into the surface or receive energy from the surface. One distinguishes between direct processes, whereupon the energy is transferred in a single collision event and indirect processes with multiple collisions. Nevertheless, when a molecule is inelastically scattered, the energy-loss of the particle is too low to allow it to stick on the surface. In contrast, some species may lack sufficient energy after the collision to escape the gas-surface potential well. If the residence time of the species on the surface is prolonged compared to the oscillation period of the particle in the potential well, the particle becomes effectively *trapped* on the surface. The fate of the trapped species depends on subsequent interactions and processes, such as whether it gains sufficient energy to escape or transitions into a state of adsorption. A measure of the probability of an adsorption event is the *sticking coefficient (S*), which gives the ratio between the number of adsorbed species and the total number of collided species. The sticking probability depends on temperature, on steric factors and a variety of other parameters such as surface coverage.[59-61]

A trapped molecule can bind to the surface in a process called *adsorption*. One form of adsorption occurs, when the colliding species bind weakly to the surface, primarily through van der Waals forces with heats of adsorption $-\Delta H_{ads}$ in the range of (20 – 30) kJ mol^{-1}: This is termed *physisorption*. The physisorbed adsorbate may be physically attracted to the surface without forming a strong chemical bond. Physisorption is often reversible, and the adsorbate can desorb easily, especially with changes in temperature. When the binding between the adsorbate and the surface is strong, a chemical bond can be established and the adsorbate may undergo changes in

its electronic structure and bonding configuration in the so-called *chemisorption*, typically with $-\Delta H_{ads}$ in the range from 50 to 400 kJ mol^{-1}.

Adsorption is typically an exothermic process, as indicated by the consistently negative ΔH of adsorption. Also, the ΔS of an adsorption process is typically also negative, because adsorption processes produce a more ordered system with fewer degrees of freedom. For a process to be thermodynamically spontaneous at constant temperature and pressure, the Gibbs free energy change (ΔG) must be negative, indicating a decrease in Gibbs energy. According to the relationship $\Delta G = (\Delta H - T\Delta S)$, will be negative when the magnitude of $T\Delta S$ is smaller than the magnitude of (ΔH) Therefore, for adsorption to occur spontaneously, the condition $|T\Delta S| > |\Delta H|$ must be met. If the $|T\Delta S|$ term increases for higher temperatures, the equilibrium will shift to desorption. On the one hand, the rate constant of physical adsorption is nearly temperature independent, since it is typically not activated. On the other hand, the chemisorption process depends on its activation energy (E_a) and the configuration of the molecule on the surface, hence, only molecules with sufficient energy to overcome the E_a and compatible configurations can be chemisorbed. The rate of adsorption r_{ads} can be expressed using a rate law that describes how quickly molecules from the gas phase are being adsorbed onto the surface. This rate law typically depends on factors such as the partial pressure of the adsorbing species and the fraction of available surface sites. Assumes a single layer of adsorption and no interactions between adsorbed molecules, the rate of adsorption r_{ads} simplifies to:

$$r_{ads} = k_{ads} \cdot P \cdot (1 - \theta) \tag{2.1}$$

where k_{ads} is the adsorption rate constant, P is the partial pressure of the adsorbing species in the gas phase, θ is the fractional coverage of the surface (i.e., the fraction of surface sites occupied by the adsorbate). The adsorption rate constant k_{ads} is typically temperature-dependent and can be described by the Arrhenius equation:

$$k_{ads} = A \cdot \exp\left(-\frac{E_{ads}}{k_B T}\right) \tag{2.2}$$

here, A is the pre-exponential factor of frequency factor, E_{ads} denotes the activation barrier for adsorption, T *is* the temperature in Kelvin and k_B is the Boltzmann constant. This Arrhenius

relationship indicates that k_{ads} increases with temperature, assuming that the adsorption process is activated. The magnitude of the activation energy provides insight into the strength of the interaction between the adsorbate and the surface; lower activation energies correspond to faster adsorption rates at a given temperature.

The coverage of a surface at the monolayer level can be described in terms of saturation coverage or one monolayer (ML). The definition of a one ML can vary depending on the reference point, whether it is with respect to adsorbate molecules or surface atoms. One ML can be defined as the complete coverage of the surface by a single layer of adsorbed molecules, with each adsorption site occupied. This definition varies depending on the size and steric interactions of the molecules, which differ across different surfaces and molecules. Another approach is to define one ML based on the number of surface atoms (e.g. 1.4×10^{15} cm^{-2} for Au(332))[50], which was also used in this work. For the latter definition, the saturation of a particular adsorbate species occurs at less than one ML, depending on the specific adsorption system.

Surface adsorbates may also diffuse across the surface. For *diffusion* on an energetically corrugated surface, the adsorbate must overcome the energetic barrier to hop from one potential well to the next one. This can lead to the adsorbate finding a more favorable site for adsorption or also desorption or for participating in surface reactions. The activation barrier for diffusion is generally lower than the activation barrier for desorption. As both processes are driven by thermal fluctuations, the surface temperature critically governs the absolute and relative rates of diffusion and desorption.

Surface reaction

Surface reactions can be classified in two main types, which are the Langmuir-Hinshelwood (LH) mechanism and the Eley-Rideal (ER) mechanism, schematically depicted in Figure 2.2. In the ER mechanism, the reaction occurs between an adsorbed molecule and a molecule in the gas phase, representing a possible, but rather rare type of bimolecular reactions. In the LH mechanism, the reaction takes place between two species, which are both adsorbed on the surface. Under UHV conditions, most surface reactions are following this mechanism, including the reactions investigated in this study. In LH mechanism, a simple example reaction such as ($A_{gas} + B_{gas} + surface \rightarrow AB$) can be described through a series of consecutive steps, which might follow the processes described above. Initially, the collision of species A and B to the surface, followed by their adsorption onto the surface.

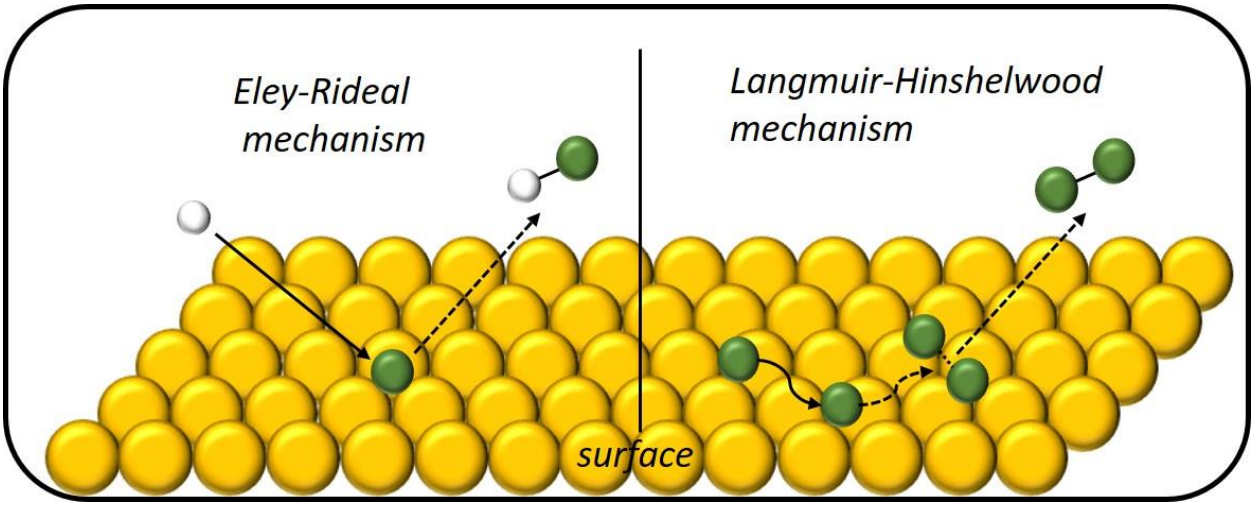

Figure 2.2: Schematic illustration of two principal ways of bimolecular reactions on surfaces: Langmuir–Hinshelwood (LH) and Eley–Rideal (ER) mechanism.

It is important to note that the term "adsorption" also applies to species that transiently reside on the surface. Subsequently, the diffused A and B undergo a reaction to form the product (AB) through an adsorbed transition state complex A-B. Finally, the resulting AB product may desorb from the surface to the gas phase. The rate of formation of a product AB (r) in a chemical reaction can be expressed as a function of the concentrations of the reactants and the reaction order. This is represented by the rate law:

$$r = k\,[A]^a\,[B]^b \tag{2.3}$$

where k is the rate constant, and a and b are the orders of the reaction with respect to reactants A and B, respectively. Arrhenius equation describes how the rate constant k of a chemical reaction depends on temperature. The rate law, incorporating the Arrhenius equation, is expressed as:

$$r = A\,exp\left(-\frac{E_a}{k_B T}\right)[A]^a[B]^b \tag{2.4}$$

where A is the pre-exponential factor or frequency factor, which represents the frequency of collisions with the correct orientation, E_a is the activation energy of the reaction. Although it might be expected that the formation rate depends solely on the surface concentration of both species, reactions on surfaces frequently demonstrate significant deviations from this simple Arrhenius-

type behavior. However, the conceptual problem with the rate equation lies in its simplifying assumptions, which may not accurately reflect the complexities of real catalytic systems. The equation assumes that the surface is homogeneous with identical adsorption sites, and that adsorbed species do not interact with each other. In reality, surfaces often have a variety of active sites with different reactivities, and adsorbate-adsorbate interactions, such as repulsion or attraction, can significantly impact the surface coverage and reaction rate. Additionally, in more complex reactions involving multiple steps, the concept of the rate-determining step (RDS) becomes crucial. The rate-determining step is the slowest step in a sequential reaction mechanism, which significantly contributes to the product formation. This crucial step can be one of the processes mentioned above such as, adsorption, surface diffusion, or limited availability of surface sites or slow reaction due to a high activation barrier. The identification of the RDS generally depends on the reaction conditions, including the concentration of reactants, temperature dependence, and the presence of intermediates or fast pre-equilibria also, as these factors determine the overall kinetic behavior of the reaction.

Competing reaction pathways add complexity to catalytic processes, making the selection of the pathway a crucial consideration. The selectivity of a catalytic reaction is governed by a multitude of factors, including the relative energies of various intermediates and transition states along different reaction pathways. Catalyst design plays an essential role in steering selectivity by providing active sites that selectively stabilize certain intermediates or promote specific reaction steps. Additionally, the kinetics of the competing reactions, influenced by factors such as, adsorption energies and surface structure, contribute to determining which pathways dominate. Understanding these intricate interactions between catalyst, reactants, and intermediates is essential for tailoring catalytic systems to achieve high selectivity towards desired products.

Desorption

An adsorbed molecule, including reaction products, can leave the surface, when the temperature of the surface and thus, the energy of the molecule becomes high enough to leave the potential well, therefore, the atoms or molecule desorbs from the surface into the gas phase. Under the assumption that all adsorbed molecule occupy identical sites and do not interact with each other, the desorption rate r_{des} is expressed by the *Polanyi-Wigner equation*[62]*:*

$$r_{des} = -\frac{d\theta}{dt} = k_n \theta^n = k_n^0 \theta^n \cdot \exp\left(-\frac{E_{des}}{k_B T_s}\right) \quad (2.5)$$

where *n* represents the order of the desorption kinetics, and k_n denotes the desorption rate constant. In *zero-order kinetics* ($n = 0$), the desorption rate is coverage independent, i.e., constant at a given temperature. While in *first-order kinetics* ($n = 1$), the desorption rate is proportional to surface coverage (θ). It corresponds to the simplest case, when single atoms desorb directly and independently of their sites. The first-order rate constant k_1^0 is measured in units of frequency, expressed as s^{-1}. In *n-order kinetics* ($n > 1$), the desorption rate is directly proportional to θ^n. This scenario typically arises in associative molecular desorption, where the desorbing molecule originates form two species residing initially at separate sites. It is important to noted that, the complicated kinetics might result in other order exponents of desorption, including fractional ones. In case of activated adsorption, the desorption energy is the sum of the binding energy in the chemisorbed state and the activation energy for adsorption, $E_{des} = -\Delta H_{ads} + E_{ads}$. Conversely, in non-activated adsorption, $E_{des} = -\Delta H_{ads}$. Note that, in general, desorption energy may depend on the adsorbate coverage, leading to more complicated relationships than the simple Polanyi-Wigner equation.

To conclude this section, the specific fate of an adsorbate is mainly influenced by the energy of the adsorbate relative to the activation energies for diffusion, (different) reactions or desorption for the specific surface. Especially, when competing pathways are accessible, a complex reaction network will govern the observed reaction kinetics.

2.1.2 Special aspects in surface characteristics and reactivity

In the previous section, the surface has been treated as a homogenous assembly of equivalent sites. However, this picture is even for well-defined flat single crystal surfaces often overly simplified. Moreover, low-coordinated sites, such as steps or kinks, may exhibit significantly different properties than sites on flat terraces.

Adsorption sites exhibit a significant influence on adsorption energy, which, in turn, can impact the activation energies associated with subsequent reactions. The strength of adsorption at these

sites critically influences the reaction kinetics by affecting the energy barrier for chemical transformations. According to the Sabatier principle, an optimal adsorption strength ensures that reactant molecules are neither too weakly nor too strongly bound to the catalyst surface. This balance is crucial because it determines the energy needed to reach the transition state, thereby directly impacting the efficiency of the catalytic process. Strong adsorption at specific sites can lower the activation energy by holding reactants in close proximity. This increased proximity promotes bond formation, thereby, accelerating reaction rates. Conversely, weaker adsorption may lead to higher activation energies, slowing down reaction kinetics. Thus, the distribution and characteristics of adsorption sites play a crucial role in modulating the energetics of catalytic processes, ultimately influencing the efficiency and selectivity of chemical reactions on solid catalysts.

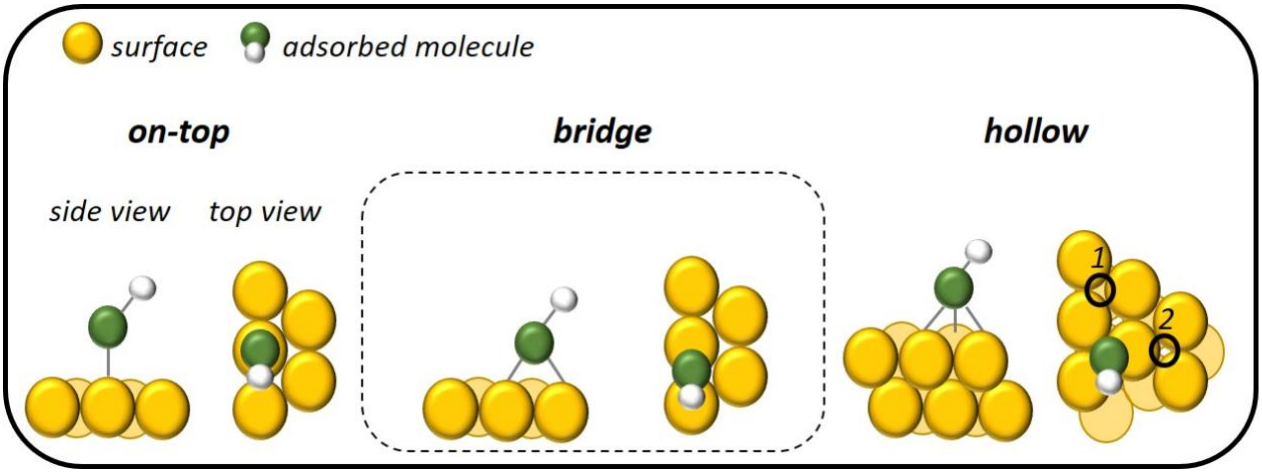

Figure 2.3: Different binding modes of a diatomic model adsorbate on metal, with (1) and (2) denoting hcp hollow site and fcc hollow site, respectively.

Even on a flat surface, different adsorption sites with varying coordination of the adsorbate can be occupied by adsorbed species. Figure 2.3 illustrates exemplarily the sites which can be occupied on (111)-surfaces of metals with face-centered cubic (fcc) crystal structure: *On-top sites*, where the adsorbate coordinates with only one metal atom, and *bridge sites*, featuring 2-fold coordination of the adsorbate. Additionally, adsorbates may also exhibit a higher coordination by adsorbing in so-called three-fold hollow sites, which can be further subdivided into hexagonal close packed (hcp) and fcc sites depending on the presence or absence of a metal atom beneath the site, respectively.

Next to well-ordered extended terraces, such as the closed-packed (111)-surface in fcc-metals, most catalysts exhibit a large number of so-called *low-coordinated sites* (LCS) referring to the coordination of the metal atoms. Figure 2.4 illustrates various types of LCS that can be present on the metal surface. LCS on a surface typically refer to locations, where an atom has fewer neighboring atoms than the atoms in an extended terrace. LCS include steps, kinks, atomic vacancies and adatoms. The coordination decreases from terrace to step to kink to adatoms. Kink, step, and terrace atoms have a large concentration on any real surface. On a rough surface, 10 – 20 % of the atoms are step sites, with about 5 % in kink sites. Steps and kinks are also called line defects, to distinguish them from atomic vacancies, or adatoms, which are called point defects.

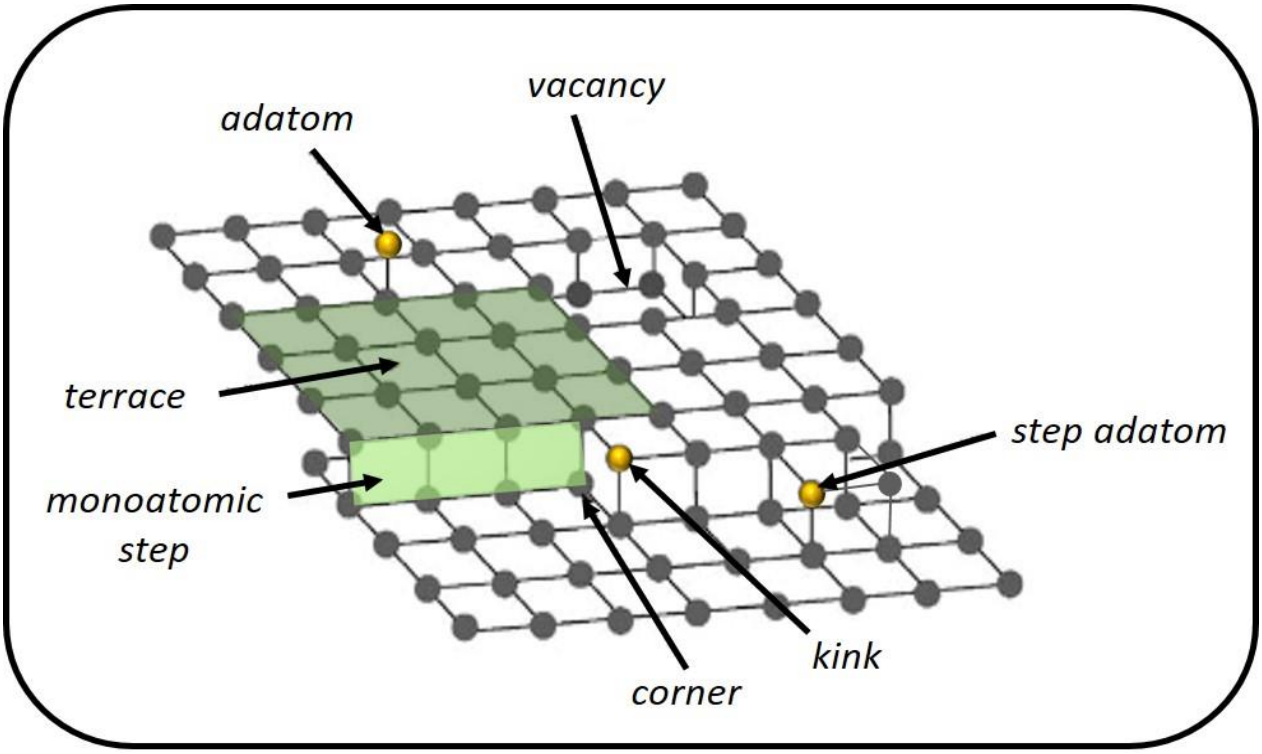

Figure 2.4: Types of structures and defects found at the surfaces of metals, adapted from ref.[63].

The reduced coordination at these sites creates energetically favorable environments for the adsorption of reactant molecules, which may influence catalytic activity and may facilitate key steps in surface reactions, as suggested, for example, in methanol oxidation on gold.[42, 50, 64] To directly investigate the role of LCS in a specific reaction, a single crystal surface oriented such that it contains a significant number of LCS (known as *stepped surface*) can be employed and compared to a surface lacking these LCS sites. In this work, this experimental approach was

applied using a stepped single crystalline Au(332) surface, featuring 6-atom wide (111) terraces separated by close packed monoatomic steps, which are aligned along the [110]-equivalent crystallographic directions. For comparison, a Au(111) surface was used. Depending on the miscut of the crystal additional LCS may be present on actual surfaces, e.g. additional kink sites may be present on Au(332).[65]

The stabilization of low index planes in metals typically involves simple relaxations, although in some cases, surface stability is not achieved through relaxation alone. To minimize surface energy, surface atoms may undergo reorganization in their bonding arrangements, resulting in *surface reconstructions.* For instance, a clean Au(111) reconstructs to the so-called herringbone structure, such that the surface contains ~ 4 % more atoms than the same plane in the bulk. The strain created by the mismatch between the top layer and the underlying bulk is minimized by zigzag arrangement.[66] The reconstruction of gold is a proof of a strong Au-Au bond, which can be explained by the increased participation of the 5d Au orbitals to the metal-metal bond.[9] In the case of gold, with its large nuclear charge, relativistic effects predict an expansion of the 5d (and f) orbitals, and a contraction of the 6s orbitals, making the 5d band a focal point of gold chemistry.[9, 67] Upon adsorption of certain gases, such as oxygen, the surface reconstruction on Au(111) is lifted, releasing gold adatoms onto the surface, which eventually agglomerate at step edges or form small Au islands.[68, 69]

Despite gold being relatively electronegative among metals, the strong charge transfer with electronegative species such as oxygen atoms presumably serves as the driving force for this process; however, the nature of the structures formed depends on the specific surface−adsorbate interaction. Surface reconstruction might influence surface reactivity since it changes the number of surface sites available to adsorption, potentially leading to a different pattern of adsorbate binding compared to the non-reconstructed surface. Consequently, the modified adsorption behavior can significantly influence reaction pathways and kinetics, impacting the overall reactivity and selectivity of the catalytic process.

2.2 Effusive molecular beams

In this section, a brief description of the effusive molecular beam (MB) techniques is given, which were applied in this work to investigate the isothermal reaction kinetics under well-defined conditions. For a detailed overview on molecular beams see references[61, 70-72]. In general, molecular beam is defined as a collision-free, spatially well-defined and directed flow of molecules.

The expansion conditions can be described by the dimensionless Knudsen number ($K_n = \lambda/d$; with λ = mean free path of the molecules and d = diameter of the orifice). *Effusive beams*, as in the present work, characterized by a large Knudsen number ($K_n \gg 1$), allow gas to expand through an orifice smaller than the average mean free path of the molecules, resulting in virtually no particle-particle collisions at the source exit. This condition allows particles entering the exit to move out of the reservoir with the equilibrium dynamic properties of the particles in the reservoir. This process is referred to as *effusion*, and the ensuing flow behind the exit is termed *Knudsen flow*. In such expansion conditions, where intermolecular collisions between gas molecules exiting the source are negligible, the energy distribution across all degrees of freedom is governed by the temperature of the stagnation state (T_0). Under these conditions, the velocity distribution of the gas molecules follows a Maxwell-Boltzmann distribution. For the flux of gas molecules (I), the Maxwell-Boltzmann distribution for velocity (v) can be expressed as:

$$I(v) \propto v^3 \cdot \exp\left(-\frac{m\,v^2}{2k_B T_0}\right) \tag{2.6}$$

The simplest design of an effusive source is a thin-walled orifice. Molecules that leave the thin-walled small orifice are distributed according to a cosine law. In order to ensure single scattering conditions, the effusive beams should minimize the number of molecules entering the UHV apparatus outside of the desired area, in this work, the sample surface. To this end, it has been found that using tubes with a large aspect ratio of length (L) over radius (r) instead of a thin-walled orifice results in a forward focusing of the effusive gas beam.[71] The collimation of such a tube can be described in terms of a so-called *peaking factor* κ, which is defined as the ratio of the total centerline flux *I(0)* relative to the centerline intensity of a cosine distribution at total flux *N*.

At low pressure, the peaking factor can be approximated as[71]:

$$\kappa = \frac{\pi}{N} \cdot I(0) = \frac{3L}{8r} \tag{2.7}$$

A spatially more homogeneous and increased total flux on the sample can be achieved, while keeping the pressure in the chamber low, if not a single channel, but an array of channels is applied. In this setup, *glass capillary arrays* (GCA) with a small diameter of the individual channels are used. To enhance the collimation of the molecular beam, two apertures are employed to filter out molecules deviating from the axis of the channels of the channel plate. These apertures are strategically connected to differential pumping stages, which utilize turbomolecular pumps to effectively eliminate the diverted molecules, thereby maintaining low pressures and ensuring transparent flux conditions. A schematic representation of an effusive beam source is illustrated in Figure 2.5. One of the advantages of effusive sources based on GCA is their greater versatility in achieving a wide range of beam fluxes, along with their low gas consumption, which is particularly beneficial when using rare or expensive reactants.

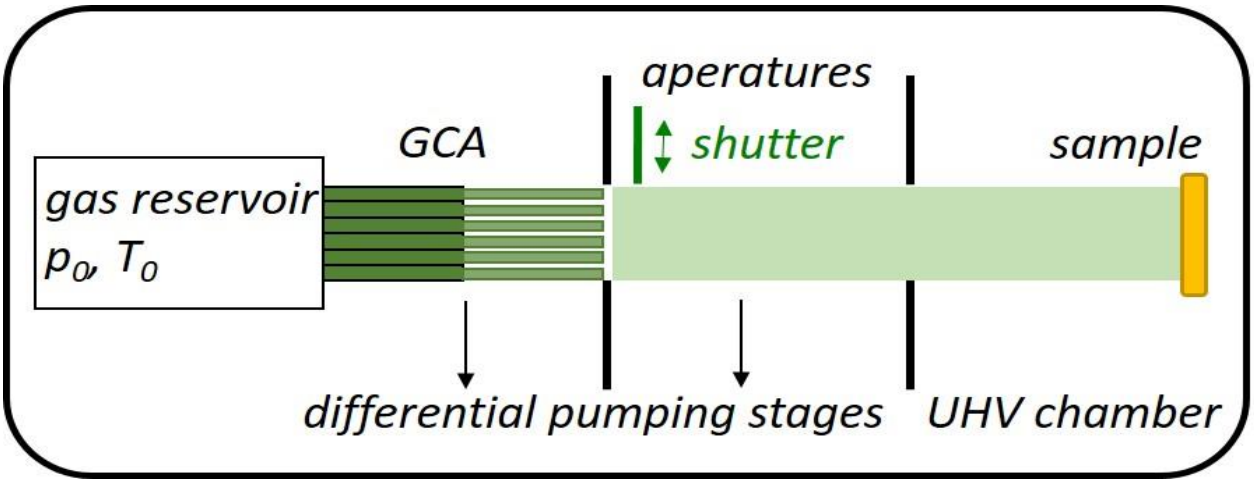

Figure 2.5: Schematical display of an effusive beam source.

Effusive MB setups present numerous advantages for investigating kinetic processes on surfaces. Firstly, they facilitate maintaining low background pressure, reducing the probability of uncontrolled collisions of these gases. Simultaneously, MB setups enable the achievement of relatively high dynamic gas pressures of reactants in the beam. This capability arises from the highly directional nature of the beams and the efficient pumping capacity of the reaction chamber.

A considerable proportion of gas particles in the MB will not impact the surface. For those that do impinge upon the surface but fail to stick, they will be rapidly evacuated. The pressure ratio between the dynamic pressure on the sample and the background pressure typically ranges between 100 and 1000. Secondly, the implementation of the first point guarantees that all particles in the beam will hit the sample surface once and only once; this is usually termed *single-collision* conditions. With this unique dynamic advantage, it becomes possible to determine absolute reaction probabilities by accounting for the effects of competing reaction and desorption processes, which wouldn't be possible under conditions at elevated pressures and ambient conditions. Thirdly, a crucial requirement for conducting kinetic experiments is the ability to exactly quantify and control the flux of reactant molecules on the sample surface, effusive beams allow for adjustment of the flux onto the sample in a large range by adjusting the inlet pressure. Lastly, molecular beams offer temporal control over the reactant flux on the surface. By employing beam flags within the beams' differential pumping stages, the beams can be shut off within hundreds of milliseconds. This capability facilitates the study of transient kinetics with high temporal resolution, in addition to investigating steady-state kinetics under continuous beam flux.

2.3 Characterization techniques

This section briefly describes the theoretical background of the characterization techniques employed in this work, including Infrared Reflection Adsorption Spectroscopy (IRAS), Time-Resolved Quadrupole Mass Spectrometry, Temperature Programmed Desorption (TPD), and Low Energy Electron Diffraction (LEED).

2.3.1 Detection of surface adsorbates by infrared reflection absorption spectroscopy

Infrared Reflection Absorption Spectroscopy (IRAS) is a technique that can be used to characterize properties of surface adsorbates. The observed vibrational frequencies not only allow to gain information on the chemical nature of the adsorbates, but also allow for characterization of the interaction with the substrate, the adsorption site, adsorption geometry or intermolecular interactions. For detailed information, see references[73-76]. A typical IRAS setup is schematically shown in Figure 2.6. The IR beam, mostly produced by thermal sources (a Globar in the case of this work), is directed by a set of mirrors onto the sample at a grazing incidence where it is partially

absorbed and the remainder is reflected onto another mirror which directs the IR beam onto the detector. A high reflectivity of the surface is required for a good signal intensity. The intensity of the IR light is not constant across the spectral range due to absorptions in the beam path caused by optical component windows before and after the sample, as well as, the characteristics of the IR source. In order to discriminate these effects from absorptions by the sample, a reference measurement needs to be taken directly before the IR experiment. In this work, the clean sample surfaces were used for these reference measurements.

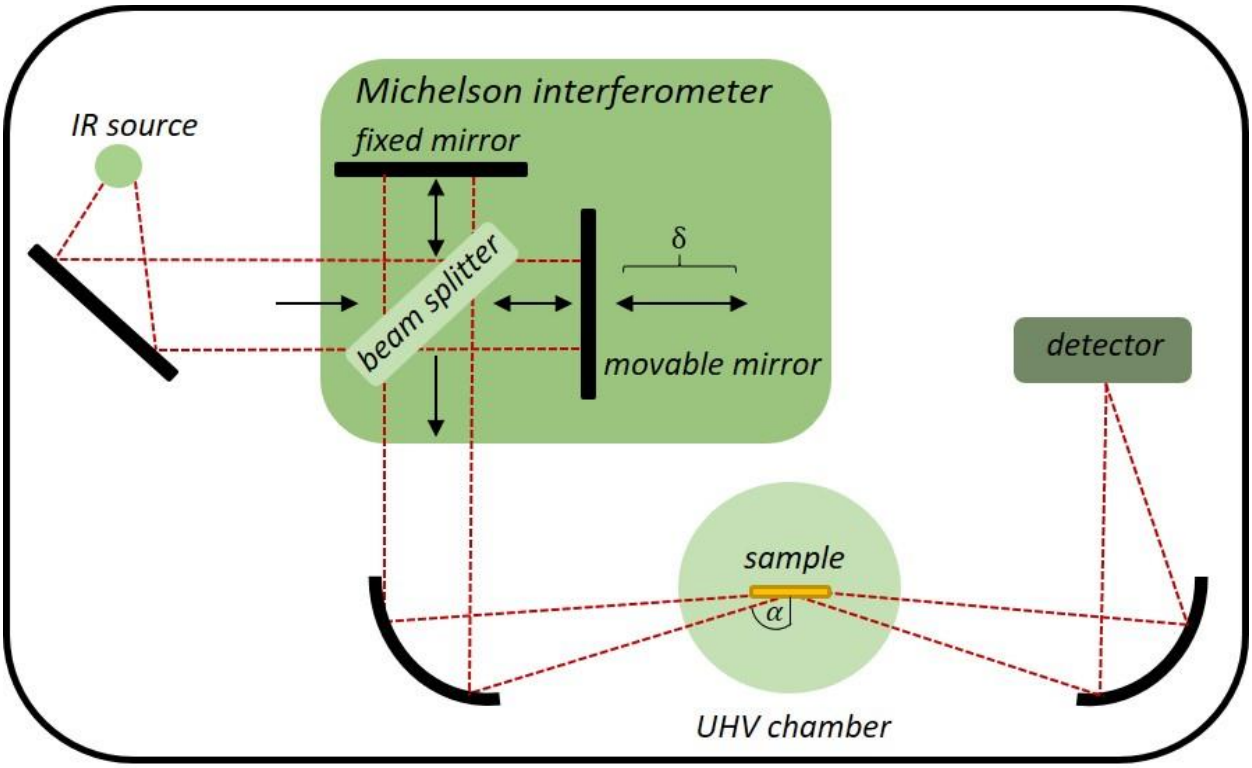

Figure 2.6: Schematic illustration of an IRAS setup indicating the important components. A representation of the working of principle of the Michelson interferometer is depicted in the inset.

The typical IRAS absorptions lie in the range of a few percent and often below, because the small number of surface adsorbates. Thus, IRAS has to detect very small amounts of substance compared to conventional transmission-mode spectroscopy. The low amount of absorber substance requires relatively long acquisition times to obtain a reasonable signal-to-noise ratio. To facilitate this, IRAS is usually performed using Fourier-Transform instruments (FT-IRAS) instead of dispersion-type instruments. In FT-IR, the full range of wavelengths interacts with the sample at the same time, and the dispersion analysis is conducted with the interference pattern caused by the mirror

movement in a Michelson interferometer; the full spectral information (reflectance intensity vs. wavenumber) is contained in the interferogram (reflectance intensity vs. path difference in the Michelson interferometer), and can be obtained from the interferogram by a mathematical procedure known as inverse Fourier transform.

For IRAS-spectroscopy on metal surfaces, it is important to consider the orientation of the transition dipole moment of the vibrations of the adsorbed molecule with respect to the metal surface, because the oscillating dipoles associated with the adsorbate vibrations induce image-dipoles in the electron distribution within the metal substrate. This image dipole and the dipole in the molecule interfere either constructively (if the transition dipole moment of the vibration is perpendicular to the surface) or destructively (transition dipole moment parallel to the surface). Thus, even if a normal mode of a molecule possesses a high transition dipole moment, the vibration mode may still be unobservable in IRAS of the adsorbed molecule on metals, if the transition dipole moment of the vibration is oriented parallel to the surface. This effect is known as *the metal-surface selection rule (MSSR).*[75] The MSSR has further important implications: For vibrations with a transition dipole moment in a direction that is not exactly parallel nor perpendicular to the surface, only the component perpendicular to the surface can interact with IR radiation on the surface and absorb energy. Thus, the IR-intensity of different vibrational modes may considerably differ from the gas phase spectra depending on the orientation of their transition dipole moment with respect to the surface.

Surface-related effects on adsorbate spectra

The molecule-substrate interaction can significantly alter creates new vibrational modes of which some are IR-active. The coupling with surface modes leads to considerable line broadening of the IR peaks as compared to gas phase peak. The interaction of adsorbed molecules with the substrate surface does also lead to *frequency shifts* in the vibrational modes of the adsorbed molecule with respect to their gas phase values: A shift to higher energies (blue shift) is due to *mechanical renormalization* by the formation of a bond to the substrate, which is a very heavy body. This is known as the *wall effect*. Additionally, the formation of the new bond can also change the electronic structure and, thus, the bond strengths of the internal bonds in the adsorbed molecule (*chemical or electrostatic effect*). The extent of this shift depends very much on the bond strength and often also on the adsorption site. Thereby, IRAS measurements of adsorbates can also be used

to probe the availability of different adsorption sites on the surface of model catalysts. In addition to the mechanical renormalization and chemical effect, another type of interaction occurs with the image dipole, which changes the electrical field at the adsorbed molecule and gives rise to a red shift of the absorption frequency; this is typically termed *coupling with the image dipole or polarization effect*.

A second group of frequency shifts is caused by adsorbate–adsorbate interactions, which increase in magnitude with higher surface coverage. The oscillating dipoles of adjacent molecules with the same or very similar vibrational frequencies, can interact directly or be mediated by image dipoles in the substrate. This *dipole coupling* typically leads to blue shifts of the observed frequencies. Additionally, the presence of a nearby co-adsorbate can induce a *chemical shift* by altering the electronic structure of the substrate. The extent of the frequency shift depends on the specific nature of these electronic changes.

The intensities of IR absorptions on surfaces are influenced by various factors, including the three following mechanisms. First, the effect of orientation to the surface due to the MSSR has already been treated in the preceding section. The second mechanism is caused by the interaction of dipoles of different neighboring molecules. The consequence for the IR spectra is an increase in the absorption intensity of the mode with higher vibrational frequency at the expense of the lower-frequency vibrational mode, which is called *intensity transfer or intensity borrowing by dipole coupling*.[77] Finally, the dynamic dipoles of the adsorbed molecules interact more and more destructively with increasing concentration of the adsorbate structure, leading to depolarization and a decrease of the spectral intensities.[77] The three aforementioned effects together lead to a more and more non-linear (and probably also non-monotonous) intensity variation with increasing coverage.

The most common limitations of IRAS include: (1) low signal-to-noise ratios, i.e. the signal may be too weak to be reliably evaluated or distinguished from the background, thus affecting the accuracy of the analysis; (2) stability of the baseline over time which is affected even by small changes in the sample position and orientation; (3) obtaining quantitative information on surface coverages based on measured IRAS intensities to estimate e.g. reaction rates; (4) distinction of chemically similar species. Despite these limitations, IRAS is a versatile and valuable tool in surface science, offering unique insights into molecular interactions at surfaces.

2.3.2 Gas phase detection by mass spectrometry

Mass spectrometry (MS) is a well-established technique for analyzing the chemical composition of a gas phase. Any mass spectrometer consists of three main components, an ion source, a mass analyzer, and a detector. In this work, quadrupole mass spectrometry (QMS) has been used for the detection of gas phase products in the pulsed isothermal MB experiments as well as for the detection of desorbing species in TPD experiments. The quadrupole is used as the mass filter, which can only be passed by the charged molecules with a specific *mass-to-charge ratio* (*m/z*). This mass-to-charge ratio can be controlled by the applied voltages to the quadrupole. For more information see also references[78-80].

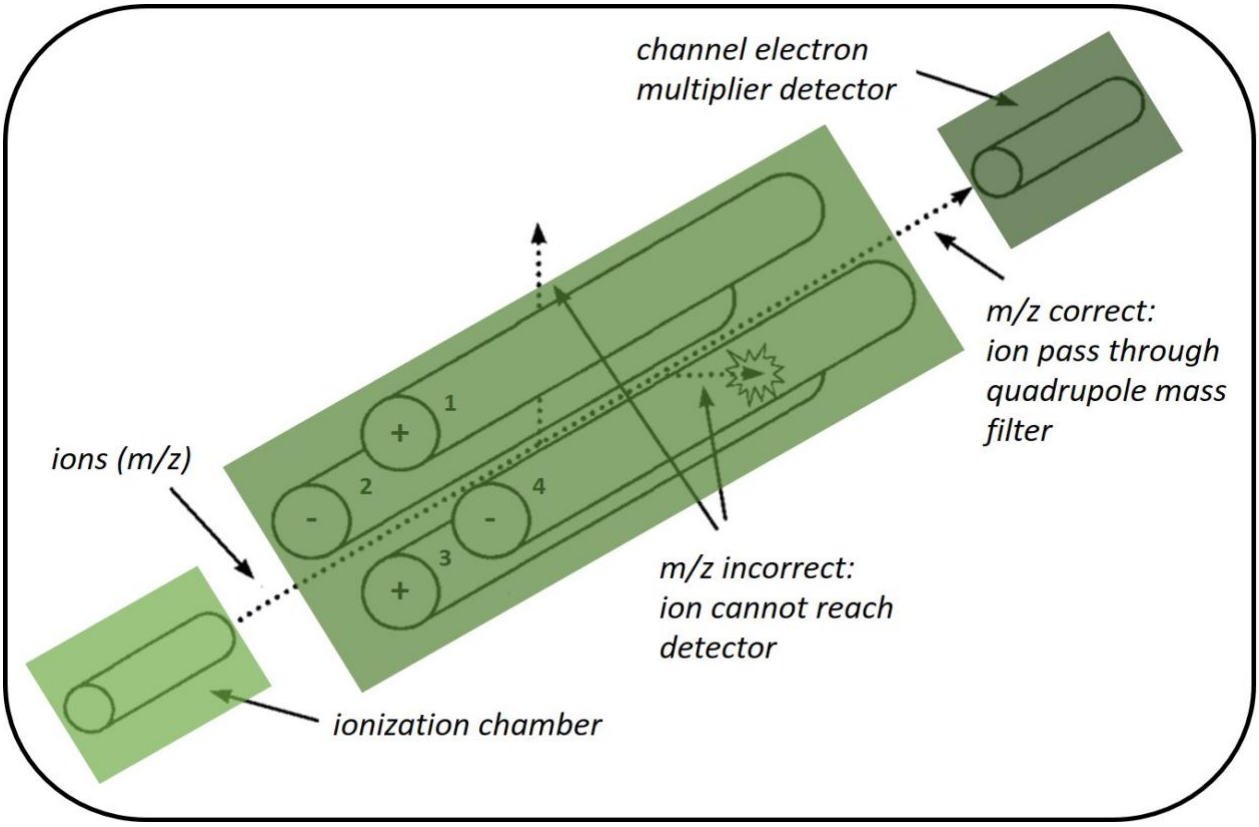

Figure 2.7: Schematic display of a quadrupole mass spectrometer (QMS) including an electron impact ion source, the quadrupole mass filter and a channel electron multiplier detector, adapted from ref.[81].

For ionization of the gas phase species, an *electron ionization* source (EI) was used, which converts the gas phase molecules into cations which are then accelerated and focused to form an ion beam

that passes into the mass analyzer. The EI source is generally composed of a cathode (filament), an ion chamber, an electron receiver, and a set of electrostatic lenses. Under ultrahigh vacuum conditions, a current is applied to the filament to emit electrons (e^-), and the electrons are accelerated from the filament to the anode. Since the fragmentation patterns and sensitivity of the mass spectrometer are influenced by electron energy, electron energies between 70 and 100 eV are typically used to optimize these factors. In this EI process, when these electrons collide with the molecules (M) in the ion chamber, the molecules are ionized (M^+):

$$M + e^- \rightarrow M^+ + 2e^- \tag{2.8}$$

This method produces not only molecular ions but also ionized fragments of the molecule. As the applied ionization energy of the electrons largely exceeds the energy required to ionize the molecules, it enables the breaking of chemical bonds and induces rearrangements, resulting in the instantaneous formation of multiple fragment ions or neutral fragments.

$$M^+ \rightarrow M^+ + N \tag{2.9}$$

After the formation of ions, they are transmitted into the *mass analyzer* and filtered according to their *mass-to-charge ratio* (*m/z*). As shown in Figure 2.7, a quadrupole analyzer consists of four long parallel rods that create a quadrupole field (ϕ). This field is established so that at any time, opposing electrodes of the quadrupole are on the same electrical potential, while the neighboring two opposing electrodes are on a potential with the same value but opposite polarity. This configuration generates a saddle potential with zero potential at the center. The potential varies over time due to an AC driver with a radio frequency (ω), typically several megahertz. One pair of opposing electrodes (1 and 3) has a constant positive offset potential, while the other pair (2 and 4) has a constant negative offset potential.

The potentials on the apex of the electrodes can be written as:

$$\phi_{1,3} = U_{const\ 1,3} + V_{amp\ 1,3} \cdot \cos(\omega t) \tag{2.10}$$

$$\phi_{2,4} = U_{const\ 2,4} + V_{amp\ 2,4} \cdot \cos(\omega t) \tag{2.11}$$

$$\text{with} \quad U_{const1,3} = -U_{const\ 2,4} \quad and \quad V_{amp\ 1,3} = -V_{amp\ 2,4} \tag{2.12}$$

During their passage in the z-direction, ions are subjected to an alternating quadrupole field in the x- and y-plane, forcing them into oscillatory paths. The AC component V_{amp} accelerates lighter ions more effectively, driving them out of the quadrupole, while the DC component U_{const} accelerates heavier ions, slowly deflecting them towards a cathode. Only ions with a specific *m/z* experience a balance of these effects, maintaining a stable path along the quadrupole's central axis and reaching the detector. Ions with unstable paths either exit the quadrupole or hit its electrodes, making the quadrupole intransparent for ions of incorrect *m/z*.

Detectors generate an electric current proportional to the abundance of incident ions, and in this setup, a *Channel Electron Multiplier* (CEM) is employed. The CEM consists of a small glass tube coated with a highly resistive material that emitting electrons and operates with an applied potential of approx. 1 to 3 kV. Electrons, accelerated towards the entrance of the negatively charged CEM, impact the surface, triggering the emission of secondary electrons that create an avalanche effect, allowing for significant amplification factors reaching up to 10^{8}.[80] While the CEM offers several advantages, it requires high vacuum conditions to prevent electric arcs, which can damage the detector. Even under ultrahigh vacuum conditions, the CEM has a finite lifetime influenced by factors such as ion impurities, electron impact depletion, and sputtering effects from ions with high kinetic energies. Additional challenges include electron-stimulated processes, electro migration, and surface oxidation, which alter the local work function and detector gain. The degradation of the detector, due to electron impacts per surface area, results in a reduction of the detector gain, limiting the total charge output to a few coulombs.

Mass resolution depends primarily on the U_{const}-*to*-V_{amp} ratio. Selecting a transparent *m/z* is achieved by changing the absolute values of U_{const} *and* V_{amp} while maintaining their ratio constant. However, heavier ions exhibit lower resolution at the same U_{const}-*to*-V_{amp} ratio compared to lighter ions. To maintain constant mass resolution across a spectrum, the U_{const}-*to*-V_{amp} ratio is adjusted for higher masses along with the absolute values of these voltages. The correlation between *m/z* and the U_{const}-*to*-V_{amp} ratio is known as the *working line*, which must be optimized for consistent instrument resolution across the mass range. Additionally, mass resolution is significantly influenced by the physical dimensions of the quadrupole rods. The diameter of the rods determines the frequency needed for a given range of *m/z* ratios, and thus impacts the overall resolution. While changing the mass transparency could theoretically be achieved by altering the AC frequency (ω),

practical instruments avoid this approach due to the complexities involved in coupling the Radio Frequency (RF) source to the transmitter (the rods). Properly tuning the impedance associated with the rods, cables, and other components is crucial to ensure effective RF coupling and maintain consistent resolution across the mass range.

Given its effectiveness, QMS provides valuable data, although it may have limitations in directly reflecting structural differences, such as conformational variations. Low mass resolution (< 3000), poor mass accuracy (> 100 ppm), and limited mass range (typically up to 3000 amu) are among these limitations.[82] Discriminating products with the same molecular mass can be intricate, relying on their fragmentation patterns, and in certain cases, observing the molecular ion may be impossible, leading to the detection of only fragment ions, which can complicate the evaluation. However, despite these challenges, QMS is highly advantageous as compared to other detection techniques in MB setups due to its simplicity, affordability, and robustness as a mass spectrometer.

2.3.3 Temperature programmed desorption spectroscopy (TPD)

Temperature programmed desorption (TPD) spectroscopy belongs to a class of techniques, in which, desorption is monitored, while increasing the surface temperature. For more information see also references[52, 83, 84]. The theoretical framework of TPD is based on the molecular-level adsorption and desorption processes (refer to *section 2.1*). If the desorbing species is produced by the reaction, a TPD experiment is often referred to as a temperature programmed reaction (TPR) experiment. In this work, TPD is used to elucidate the energetics of the interaction between the adsorbate and the surface. Furthermore, TPR experiments were used to identify different reaction channels and compare with other model studies. A TPD/TPR experiment is consisted of the following steps: (1) adsorption of the adsorbate(s) on the sample, typically at low temperature, (2) heating the sample with a temperature program $\beta(t) = dT/dt$ (with the temperature T usually being a linear function of the time t), (3) detection of the desorbed gas by a QMS as a function of the surface temperature, the sensitivity of the measurement can be increased by means of a so-called *Feulner cup*, which can increase the fraction of species being detected with the QMS, illustrated schematically in Figure 2.8.

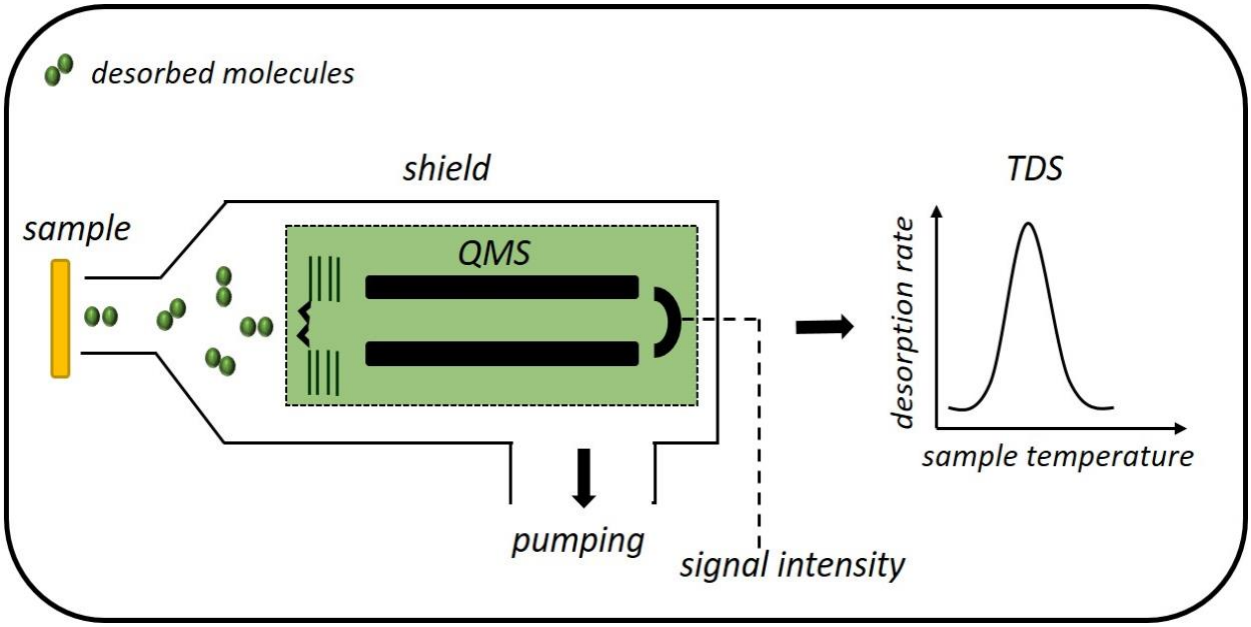

Figure 2.8: Schematic setup of the temperature programmed desorption spectroscopy measurement. A shielded and differentially pumped QMS detects desorbing gas from the heated sample, adapted from ref.[84].

The obtained data, in the form of Temperature Desorption Spectra (TDS), are presented as the variation of detector signal intensity, which is proportional to the partial pressure of the species in the gas phase, plotted on the y-axis as a function of sample temperature (or time) plotted on the x-axis. The analysis of TPD spectra can provides valuable information on the kinetics of adsorption and desorption reactions on surfaces. Ideally, reaction order and activation energy can be obtained from the position, width, and displacement of desorption peaks under varied coverage and heating rate. The position of the peak maximum (T_{max}), representing the temperature at which r_{des} is maximized, correlates with the activation energy for desorption (E_{des}). Generally, a higher T_{max} value indicates a stronger interaction between the adsorbate species and the surface. For the simplest case first-order molecular desorption, the heat of adsorption – ΔH_{ads} typically equals the E_{des}, assuming negligible activation energy for adsorption. Consequently, T_{max} is also linked to – ΔH_{ads}, i.e., to the strength of adsorbate binding to the surface.

The analysis of the TDS data also involves the application of various kinetic models to extract quantitative information about the desorption processes. *Zero-order kinetics*, such as desorption of multilayers, is characterized by an increasing desorption temperature with increasing coverage.

The spectra exhibit a consistent leading edge, and desorption rate remains constant during the process, depending primarily on the adsorbate properties rather than on the amount of the surface coverage. The influence of the surface is almost completely screened in this regime. The bonds in the second and subsequent monolayers are usually weaker than the bond of the first monolayer to the substrate, therefore, multilayer desorption peaks appear at lower temperatures relative to the desorption peaks from the first monolayer. Conversely, for *first-order kinetics*, the corresponding expression does not involve the coverage, and the desorption rate is directly proportional to the number of adsorbed species on the surface. Conducting a series of measurements with different initial degrees of coverage (coverage-dependent measurements) yields curves with identical temperatures at their maxima. In the case of n^{th}*-order kinetics*, where n > 1, non-linearity is introduced into the desorption process. Unlike first-order kinetics, desorption temperatures are influenced by the coverage of adsorbates on the surface.

The adsorption temperature (T_{ads}) is also influencing the shape of TPD profile, since it determines the initial state of adsorbate-surface interactions and the distribution of adsorbed species on the surface. Desorption occurs subsequently to adsorption due to thermal motion, where kinetic energy is sufficient to break the bond between the adsorbate and weak active sites. At higher T_{ads}, molecules desorb more readily, resulting in simpler TPD profiles with single peaks or less overlap, with desorption profiles shifted towards higher temperature regions. Conversely, at lower T_{ads}, more adsorption sites are occupied, leading to complex TPD profiles with multiple overlapping peaks as molecules desorb from sites with varying binding energies.

In conclusion, desorption methods are valuable techniques to determine desorption energies in case the adsorbate does not undergo reactions. As a kinetic experiment, precisely extracting the energetics requires considerable effort, as multiple spectra under various conditions must be measured and consistently analyzed. In complex reactive scenarios, it is often necessary to combine TPD experiments with other methods to accurately determine the thermodynamic parameters of surface species and to interpret the results effectively.

2.3.4 Low energy electron diffraction

Low Energy Electron Diffraction (LEED) is a surface sensitive diffraction technique to investigate long-range order of surfaces, which provides information on periodic structural features of the sample surface. For detailed information see reference[85]. In this work, it has been employed primarily to assess the well-ordered and reproducible characteristics of gold crystal surfaces following the cleaning process. A schematic of the working principle for LEED is shown in Figure 2.9. The experiments are typically conducted under UHV conditions to ensure well-defined surfaces without undesired adsorbates and to avoid unwanted collisions of the electron beam with gas phase molecules. The de Broglie wavelength of an electron is given by:

$$\lambda = \frac{h}{\sqrt{2\,m\,E}} \tag{2.13}$$

where h is Planck's constant, m is the mass of the electron, and E is the kinetic energy of the electron. In the typical range of energies used in LEED (30 – 200 eV) the electrons have a wavelength (~ 1 – 2 Å), which matches the length scale of interatomic distances in solids. Electrons with energy in this range have a mean free path in solids of only a few atoms. This means that, elastically scattered electrons forming the diffraction spots will originate from a few layers closest to the sample surface. Thereby, LEED allows probing of the long-range order of an ordered surface through diffraction experiments.

The technique relies on a mm^2-sized electron beam (1) with a well-defined energy, impinging onto a surface. The diffracted electrons (2) are observed in reflection geometry. They travel in the field-free space between the sample and the first grid of the hemispherical grid analyzer (4) (sample and first and last grid of the analyzer are grounded). The grid in the middle of the stack (in many LEED optics two grids are used) establishing the analyzer (4) is set to a potential such, that only elastically scattered electrons pass through the outer grid (also grounded), while all others are repelled. The electrons passing through the outer grid are accelerated onto a fluorescent screen (5) resulting in a diffraction image in case of a well-ordered surface, as shown in Figure 2.9 (b, c).

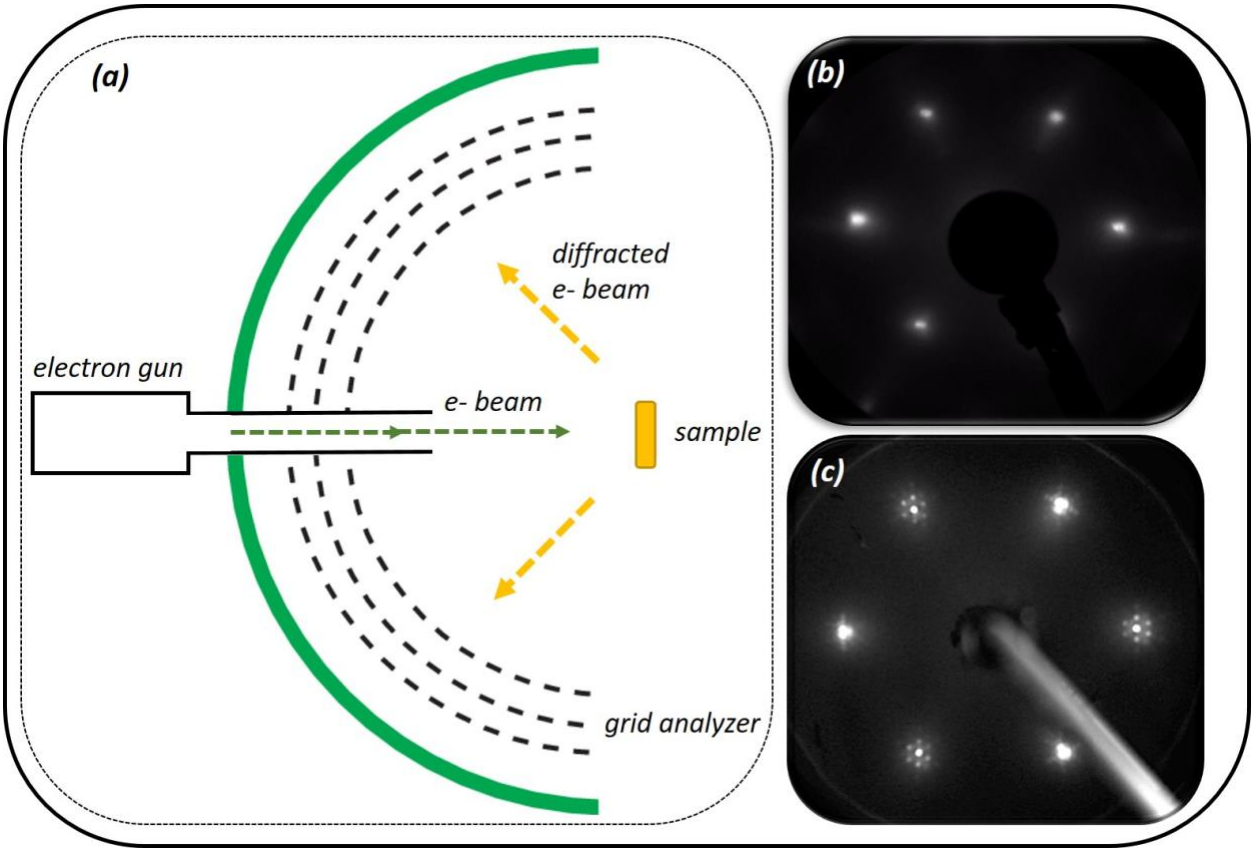

Figure 2.9: (a) Schematic of LEED working principle, (b) LEED patterns of hexagonal (1x1) unreconstructed Au(111) surface, taken at an electron energy of 200 eV (contrast inverted) and (c) LEED patterns corresponding to the (22x√3) reconstructed Au(111) surface, adapted form ref.[86].

The LEED pattern represents a *reciprocal space image* of the surface, whose resolution is -apart from other experimental aspects- limited by the *coherence length* of the electron beam. If the electron gun operated as a monochromatic point source, this coherence length would equate to the size of the incoming electron beam. However, due to the non-monochromatic nature of the source, the radiation is not completely in phase over the full extent of the beam. There exists a threshold for how much the radiation can be out of phase while still producing coherent scattering, defining the maximum coherence length. For conventional electron beams the coherence length $\leq$ 10 nm. Hence, LEED is not sensitive to disorder on length scales > 10 nm. Despite this limitation, diffraction techniques are proficient at finding order even when it is mixed with disorder.

Figure 2.9 (b), shows a LEED pattern unreconstructed Au(111) surface. The sharply defined diffraction pattern exhibits a hexagonal symmetry, which is characteristic for the (111) oriented

surface of a fcc crystal. In Figure 2.9 (c), as Au(111) is the only (111) crystal face of all the chemical elements with a fcc structure, that undergoes reconstruction under UHV conditions. The corresponding LEED pattern of the reconstructed Au(111) surface exhibits spots associated with the signature Au(111)-(22x$\sqrt{3}$) "herringbone" reconstruction pattern.

Upon inspection of the LEED pattern, the qualitative estimation of the surface's structural quality can be conducted. A clean well-ordered surface exhibits bright, sharp spots with low background intensity. Conversely, impurities, structural defects or crystallographic imperfections exhibit broadened and weakened spots, accompanied by increased background intensity. Increasing surface temperature is also associate with increased background due to increase in the vibrational motion of the surface layer, which results also in a decrease in the intensity at the reflex maximum. The appearance of additional spots in the LEED pattern typically indicates surface reconstruction, adsorption of foreign species, superstructures, multiple domains, or surface defects. It is important to note that scattered waves interfere to produce a diffraction pattern, only when they originate from the same surface region not larger than the coherence length. If the size of the superstructure domains exceeds the coherence length, the resulting LEED pattern represents a superposition of diffraction patterns from separate domains.

2.4 Methanol (partial) oxidation on single crystal gold surfaces

As previously outlined in Chapter 1, the aim of this work is to enhance the microscopic understanding of the surface processes on np-Au catalysts during the oxidation of methanol. Therefore, previously reported results from literature relevant to this work are presented in the following section. This entails both results obtained for applied np-Au as well as for model studies under well-defined conditions. For reactivity investigations of model systems, aside from a limited number under isothermal conditions[50, 51], mostly TPR measurements have been performed thus far. It is important to note that molecular oxygen does not dissociate under UHV conditions on Au surfaces[87], thus, all model studies require a source of reactive oxygen, such as ozone[30, 88] or oxygen atoms[49, 89, 90]. In contrast, for the aerobic oxidation of methanol on np-Au with molecular oxygen, the activation of the oxygen molecule occurs on residual Ag or Cu and is for these systems the rate limiting step.[35, 40]

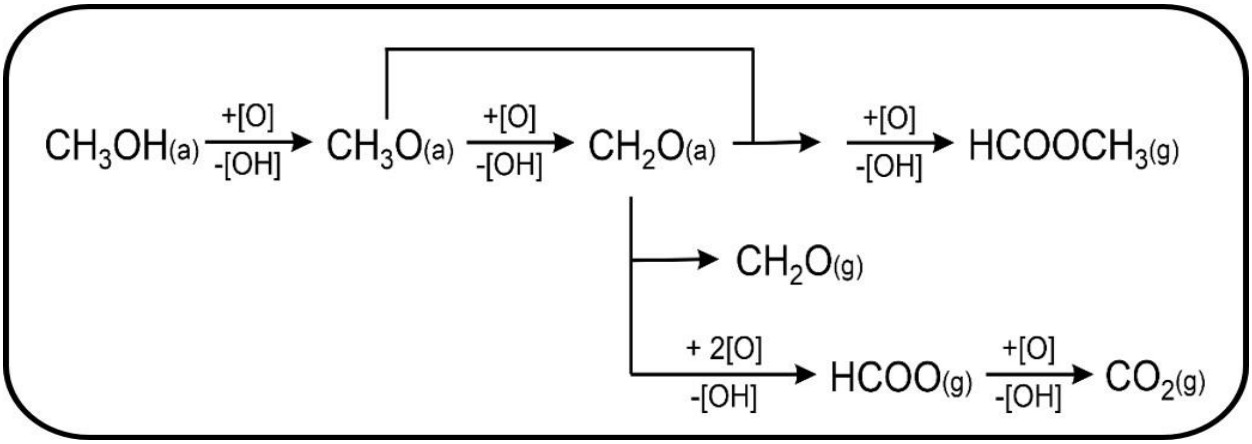

Figure 2.10: Simplified reaction network for the partial oxidation of methanol on Au and competing reaction pathways i.e. desorption the corresponding aldehyde and overoxidation of aldehyde to carboxylate and subsequently CO_2, adapted from ref.[50].

Based on a series of TPR studies and high-resolution electron energy loss spectroscopy (HREELS) of methanol on oxygen pre-covered Au(111), a reaction mechanism for methyl formate (MeFo) formation from methanol oxidation with activated oxygen has been proposed,[28-30] as schematically depicted in Figure 2.10. As a first step, the O-H bond in methanol is selectively activated by surface adsorbed activated oxygen, which acts as a Brønsted base so that adsorbed methoxy species form. Subsequently, the dehydrogenation of methoxy leads to the formation of formaldehyde, which is considered to be the rate limiting step in the presence of activated oxygen, as deduced from TPR experiments, where co-adsorption of formaldehyde and methanol resulted in a reduced reactive desorption temperature of MeFo.[28, 30] The formation of MeFo involves a reaction of formaldehyde with an adsorbed methoxy species to form a hemiacetal, undergoing oxidative dehydrogenation, resulting in MeFo. The formation of MeFo is competing with other reactions: On the one hand, formaldehyde may desorb before reacting with a methoxy and oxygen to MeFo, which limits MeFo formation under single collision conditions.[50, 51] On np-Au, on the other hand, formaldehyde may collide with the catalyst surface many times before exiting the reactor bed. Therefore, desorbed formaldehyde may undergo subsequent reactions and thus contribute to the MeFo yield in np-Au. Accordingly, short contact times, which correspond to a limited number of surface collisions, result for np-Au in a higher formaldehyde formation and a lowered MeFo selectivity.[35] Apart from desorption, formaldehyde may undergo overoxidation, resulting in formate species and subsequently in CO_2 formation. In agreement with np-Au studies, TPR as well as pulsed isothermal

MB experiments show an increase in overoxidation products for increasing oxygen coverage or flux.[30, 51] Yet, not only the amount of oxygen, but also the type of oxygen species were suggested to affect the selectivity: Using scanning tunneling microscopy (STM), different types of oxygen species, such as small disordered oxygen islands or oxidic phases (corresponding to a well-ordered multi-dimensional Au_xO_y-phase), have been identified even at low coverage on low-index Au surfaces and have been reported to differ in reactivity in TPR experiments, also depending on the size of the oxygen islands.[12, 35]

For surfaces with low-coordinated sites (LCS), theoretical calculations indicate a preference for oxygen adsorption on these sites. Accumulated oxygen at steps is suggested to favor overoxidation to formate, while atomic-oxygen, present during oxygen-pulses, enhances the formation of MeFo.[33] Isothermal pulsed MB experiments on the stepped Au(332) surface, exhibiting a high number of LCS, employing a flux of atomic-oxygen, provided evidence for various oxygen species on the stepped surface, differing in their reactivity towards the competing reaction pathways.[50, 51, 64] In isothermal MB experiments at 230 K, MeFo formation was found to proceed predominantly during atomic oxygen exposure, with higher formation rates at LCS. In contrast, unwanted formate formation increased after oxygen pulses, suggesting that this reaction proceeds efficiently with residual and, thus, presumably accumulated oxygen. Moreover, no indication for a preferential formate formation at step sites was found. The subsequent decomposition of formate was feasible with atomic oxygen already at 230 K in the isothermal MB experiments. While in TPR experiments, where mainly accumulated oxygen is expected, which demonstrate less reactivity than atomic oxygen, a higher surface temperature is required for this reaction. Moreover, the unwanted overoxidation of the partial oxidation product MeFo was connected to specific oxygen species at a subset of low-coordinated surface sites: TPR measurements showed that these species allow for the MeFo overoxidation at low temperatures and even at low oxygen coverages, which are typically connected to a high selectivity to MeFo and not with overoxidation.[91] Yet, in isothermal MB experiment, the reaction was slow, which was attributed to a limited availability of these specific species. This explains how a high MeFo selectivity can be achieved on np-Au even at high conversion, where the MeFo content in the feed is significant and could therefore compete with methanol oxidation. To this end, these measurements suggested the importance of LCS and the specific oxygen species associated with them. However, there is a lack of direct comparison with systems without the LCS.[50, 51, 64, 91]

Next to MeFo, formaldehyde or CO_2, the oxidation of methanol also yields water as a product. Consequently, the water content in the gas phase in the np-Au reactor bed will increase with increasing conversion. Although water exhibits weak adsorption on Au surfaces, OH species may transiently form in the presence of activated oxygen.[90] The OH species differ in their reactivity from oxygen species, e.g. OH may accelerate oxidation reactions by changing the stability of oxygen islands, facilitating CO oxidation, even at low temperatures as 77 K.[44, 45, 92] In contrast, for liquid phase methanol oxidation on np-Au, a detrimental effect of water on the MeFo selectivity was reported, presumably by favoring the formation of methyl diol.[46] Also, theoretical calculations for methanol oxidation on Au suggest a different reactivity for OH species as compared to atomic oxygen, which exhibit higher activation barrier.[93] In contrast to reports suggesting that water has a negative effect on MeFo formation, high selectivity for MeFo at high conversions, and therefore, high water content, has been observed in gas phase methanol oxidation on np-Au. Despite this apparent discrepancy, there has been a lack of model studies under isothermal conditions that could clarify the role of by-product water in methanol oxidation. Addressing this effect under well-defined conditions could provide valuable insights into the reaction mechanism.

3 Experimental details

In the following section, selected experimental details of the measurements performed in this work are described. In 3.1, a brief description of the molecular beam setup is given. Further experimental details and key considerations specific to the experiments in this work are elucidated in 3.2.

3.1 Experimental setup

3.1.1 Molecular beam apparatus

The experiments were conducted in a molecular beam setup, which is designed to study isothermal reaction kinetics on single crystal surfaces in a well-defined manner using molecular beams (MB) and combine this information with spectroscopic information on the surface species present during the reaction by means of in-situ IR spectroscopy. The setup was built prior to this thesis and has been described in detail by Moreira.[94] In brief, the apparatus is set up by two main chambers, which are separated by a manual gate valve and are named as preparation chamber and scattering chamber. The ultra-high vacuum (a base pressure of approx. 1×10^{-10} mbar) is measured by means of ion gauges (350 UHV Gauge, Granville Phillips) and maintained by turbo-molecular pumps (Turbovac 350i, Leybold (preparation chamber) and TMU 521 P, Pfeiffer (scattering chamber)) which are connected to rotary vane pumps (Duo 5 M, Pfeiffer). A long travel manipulator of 600 mm (HPLTC 60, Vacuum Generators) with a differentially pumped rotary feedthrough is used to transfer the sample between the chambers and to manipulate the sample position along/around four axes (X, Y, Z and θ).

The preparation chamber is equipped with a sputter gun (IQE 11/35, SPECS) for sample cleaning, a low energy electron diffraction (LEED) system (LEED/Auger unit, Omicron) for testing the long-range order of the sample surface, and a quadrupole mass spectrometer (Balzers Prisma QME 200 BGD28510) equipped with a Feulner cup to enhance sensitivity (see Figure 3.1) for temperature programmed desorption/reaction (TPD/TPR) measurements. In the scattering chamber, two effusive molecular beams (MB), based on a design introduced by Libuda and co-workers,[95] are employed to expose the surface with educts, a leak valve (UDV 035, Balzers) was

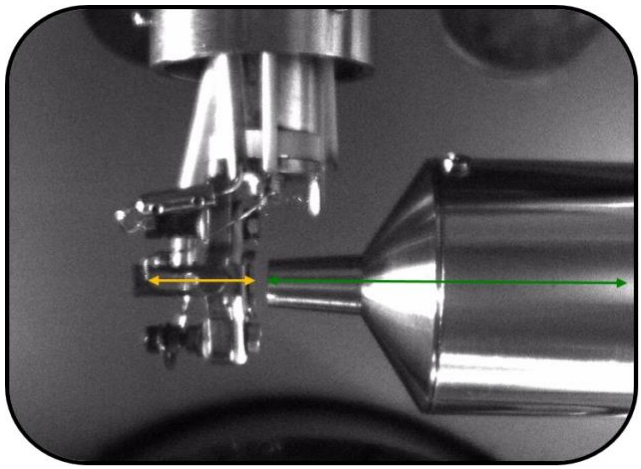

Figure 3.1: Photo depicting the experimentally used setup for TPD measurements. A green arrow marks the Feulner cup, while the yellow arrow indicates the placement of the sample.

used in some experiments to dose educts, when significantly lower dosages were required than are achievable with the MB. As gold does not activate molecular oxygen, as mentioned earlier, a thermal atomic oxygen source (Dr Eberl MBE Komponenten GmbH), also known as the oxygen cracker, is used with a pin-hole doser to generate a precisely focused effusive beam composed of atomic oxygen directed at a 45° angle toward the sample. It is equipped with an iridium (Ir) capillary connected to the gas inlet and whose inner surface allows to split O_2 at high temperature. To generate a precisely focused effusive beam of atomic oxygen, transparent flux conditions are introduced by placing a 50 µm pinhole in front of the gas inlet of the oxygen cracker. A stagnation flow monitor with a high precision ion gauge (360 Stabil-Ion, Granville-Phillips) mounted on a xyz-manipulator is used to measure the pressure in front of a small (1 mm diameter) orifice. A proper positioning of the orifice allows to map the spatial distribution of the flux of the effusive beams at the sample position. The temporal evolution of gas phase species during pulsed MB experiments is followed by a quadrupole mass spectrometer (MAX-500HT, *m/z* range of 1 – 500 amu, Extrel). To monitor surface adsorbed species during the pulsed MB experiments, in situ IRAS measurements were conducted in grazing reflection geometry applying an IR spectrometer (IFS 66v/S, Bruker) with an MCT detector. The scattering chamber is also equipped with a flag made of non-sticking material (quartz plate) of 12 mm diameter to shield the sample from molecules effusing from the MB sources. The effusive beam sources can be modulated by automated valves and shutters, while the leak valve requires manual operation. The inlet pressure of the beams is adjusted by flow controllers (MKS, Type 250) and the corresponding valves. In addition, the flux of the beams, the temperature of the sample as well as the mass spectrometer and the IR-setup can be automatically controlled. Automation of the experiments allows for a fast and exact modulation of the molecular beam flux. It ensures a high reproducibility and thus enables a direct comparison of different measurements in one series.

3.2 Experimental considerations

3.2.1 Exposure by effusive molecular beams

Prior to conducting isothermal pulsed MB measurements, particular attention to achieving a stable, reproducible and contaminant free exposure of the clean sample with the desired reactants was paid to ensure reproducible results in these kinetic measurements.

For achieving a reproducible and stable flux of oxygen atoms, the oxygen source with the heated Ir-tube was flushed with oxygen at the beginning of the measurement day for at least 1.5 h applying the highest used inlet pressure planned for this day. Additionally, the oxygen source is flushed with oxygen gas for at least 15 min between different measurements. This flushing procedure was applied to remove any carbonaceous deposits which may accumulate in the absence of gaseous oxygen on the hot Ir-tube, when organic molecules, such as methanol, are dosed into the scattering chamber, and which may by reaction with oxygen lower the flux of atomic oxygen onto the sample.

The effusive MBs, used for supplying methanol or water, were flushed, i.e. the desired gaseous molecules were introduced into the scattering chamber, for at least 3 h, when a new type of reactant was used in the specific MB. During this flushing, a high inlet pressure was chosen. This procedure was introduced to desorb contaminants from the walls of the scattering chamber, the differential pumping stages of the MBs and the high vacuum parts of the MBs, before starting experiments with the new reactant. Thereby, unwanted exposure of the sample with impurities desorbing from these walls in the presence of the new reactant can be minimized.

Although high-purity methanol was utilized in the experiments, each batch of methanol carries distinct impurities that influence surface reactivity and selectivity toward methyl formate (MeFo), and the appearance of species containing C-H bonds in IRAS. Previous studies have indicated that certain unknown contaminant strongly binding to the Au(332) surface, thereby preferentially blocking numerous highly reactive sites for MeFo formation, particularly under methanol-rich conditions.[50] Experimentation with various methanol batches has revealed that measurements conducted with the current type of methanol (Honeywell Riedel de Haën, Chromasolv, ≥ 99.9 %) exhibit less pronounced MeFo deactivation and reduced IRAS contamination. Furthermore, to further minimize impurities that could block active sites for methyl format formation, the flag is positioned as close as possible to the crystal surface while ensuring sufficient distance to enable

IRAS measurements during the stabilization of the QMS signal before the oxygen pulse. Between measurements, the sample was heated *in vacuo* for a short time (i.e. flashing) to 800 K to ensure desorption of adsorbates which may remain e.g. after an isothermal, pulsed MB measurement on the surface, such as non-reacted activated oxygen. Heating to significantly lower temperatures (500 K) resulted in non-reproducible results indicating incomplete desorption of surface adsorbates.

3.2.2 Detection of gas phase species by time-resolved quadrupole mass spectrometry

For monitoring the evolution of the gas phase species in pulsed isothermal MB experiments by time-resolved mass spectrometry (QMS), special precautions were taken to achieve stable and reproducible results. In these isothermal MB experiments, on the one hand it is desirable to monitor the flux of reactants to ensure that these agree with expectations. On the other hand, the product formation in the gas phase is to be followed to investigate their kinetics. While the flux of reactants, such as methanol, is typically chosen to be high to ensure sufficiently high transient surface concentrations and thus reaction rates, the flux of formed gas phase products is significantly lower and limited by the amount of oxygen atoms in the partial oxidation reaction discussed in this thesis. Additionally, product signals may coincide in *m/z* ratio with that of predominant residual gases in UHV chamber (e.g. H_2O, and CO_2). When choosing the sensitivity settings for the QMS, this large discrepancy in the corresponding signal intensities may cause experimental issues. If the sensitivity is chosen too low to accommodate the high signals of reactants or some residual gases, the signal to noise ratio may be too low to allow for detection of weaker product signals preventing their detection. However, choosing a high sensitivity may result in too high-count rates (exceeding 1×10^4 [cts/s]) which can affect the performance of the channeltron detector, i.e. the signal intensity may show a declining trend over time, rendering such measurements unusable. To minimize such effects when choosing a high sensitivity to allow for analysis of weak product signals, the measurement of high intensity signals on specific *m/z* ratios (e.g., 18, 30, and 45) was excluded, despite the potential insights they may offer. For monitoring the reactant flux, instead, a *m/z* ratio of a less abundant isotopologue was chosen for detection to limit the count rate. Figure 3.2 shows QMS intensity of methanol where instead of *m/z* 32 corresponding to $^{12}C^{1}H_3{}^{16}O^{1}H^+$, i.e. the parent ion of the containing only the most abundant isotopes, *m/z* of 34 was used for detection, i.e. here several exchanges to less abundant isotopes, such as ^{13}C, ^{2}H or ^{18}O, need occur limiting the signal

intensity on this *m/z* ratio significantly. It can be seen that even on *m/z* 34 a good signal to noise ratio can be achieved. Moreover, a comparison of the signals taken approx. 1 year apart under comparable methanol flux conditions reveals only minimal degradation of the detector over the course of a year and proves this strategy successful for maintaining long-term stability of the MS required for achieving reproducible results and eliminating the need for extensive data corrections due to QMS detector instabilities, making the comparison between sets of data is straightforward. Please note that upon the introduction of methanol beams into the UHV chamber, there is an initial exchange with the residual gases adsorbed on the walls, which takes some time before reaching a steady state. This phenomenon accounts for the observed deviation from the rectangular shape in the QMS signal of *m/z* 34.

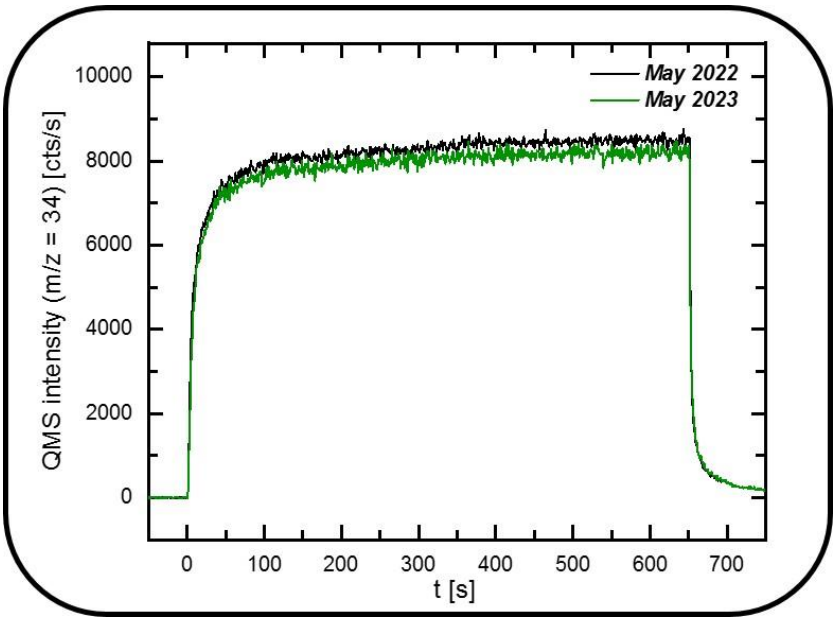

Figure 3.2: QMS intensity of methanol by monitoring m/z 34 obtained under the same methanol flux conditions in two different years.

For MB isothermal measurements, Figure 3.3 illustrates exemplarily one-pulse methanol oxidation measurements, first the background signal intensity of the chamber was recorded for couple of seconds (about 160 s in case of Figure 3.3, indicated by dashed gray line at time zero, t = 0 [s]). Next, methanol was introduced into the chamber (indicated by dark green dashed line in Figure 3.3(a)), while the flag was placed in front of the sample to prevent methanol from directly impinging onto the gold surface. After allowing the partial methanol pressure to rise for 150 s to a steady state in the chamber, the flag was removed from the beam path allowing methanol and

oxygen to strike the gold surface and thereby for formation of MeFo *m/z* 60 for 200 s, the oxygen pulse (O-pulse) indicated by the gray box. After the end of the O-pulse, exposure to methanol was continued for 300 s. At the end of this one-pulse experiment (typically 500 s after flag removal), the beams are closed, and the flag is repositioned in front of the sample.

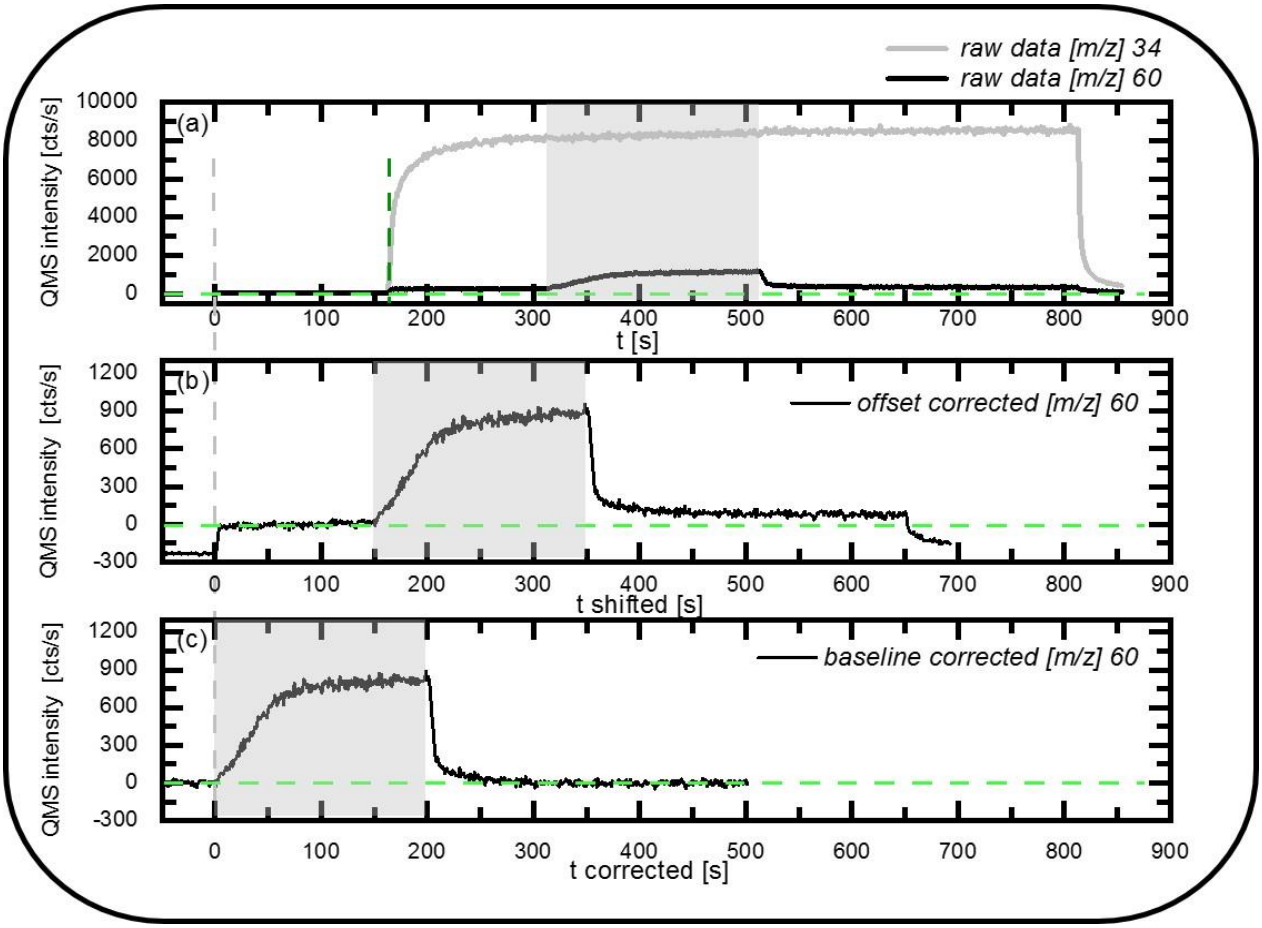

Figure 3.3: QMS intensity of methanol and methyl formate by monitoring m/z 34, and 60, respectively, obtained during isothermal MB one-pulse methanol oxidation. Raw data in (a), offset corrected and time shifted data in (b), and baseline corrected, and time corrected in (c).

The raw QMS data obtained from the Merlin Automation Data System Software undergoes processing to render it usable, involving a series of corrections. Initially, the evolution time of *m/z* 34 (indicated by the dark green dashed line) is utilized to adjust the time axis for *m/z* 60. Specifically, the time axis in Figure 3.3(a) is subtracted by approximately 160 s to obtain the shifted time axis in Figure 3.3(b). Furthermore, the QMS intensity of *m/z* 60 is shifted by about 230 [cts/s] to ensure that the baseline before the O-pulse typically starts at zero. As it is noticeable

that the baseline after the oxygen pulse in Figure 3.3(b) is also non-zero, the baseline is further corrected using home-written software by assuming that at the end of the O-pulse, no further *m/z* 60 formation occurs. Finally, Figure 3.3(c) depicts the version of the data utilized for evaluation, featuring baseline-corrected data, with time further shifted by 150 s to align the start of the measurement with the O-pulse.

4 Summary of the papers

In this work, the (partial) methanol oxidation on gold surfaces was investigated under well-defined single collision conditions using a molecular beam approach and employing single crystal surfaces as model catalysts to address previously scarcely investigated questions concerning the catalytic properties of nanoporous gold (np-Au). One focus was on the role of low-coordinated sites (LCS) in the selectivity towards desired methyl formate (MeFo) formation as well as in the unwanted overoxidation. This aspect is closely related to the heterogeneous speciation of oxygen on the gold surfaces on their influence on reactivity and selectivity in methanol oxidation. The results of these investigations were published in two papers (i. e. [I - II], see Chapter 6). Additionally, the effect of water on the selectivity in methanol oxidation was studied, as water is a product of the methanol oxidation as well as a common impurity in the (methanol) reactant feed and may affect the reactivity in applied gold catalysts. The results are published in an additional paper further demonstrating the importance of LCS as well as different oxygen species. In this chapter, the findings of the three publications are summarized to highlight their interconnection and show how they further complete the understanding of oxidation reactions on gold catalysts.

The (partial) oxidation of methanol on single crystalline gold surfaces was investigated using isothermal, pulsed MB experiments under single collision conditions which allow to study the reaction kinetics under well-defined fluxes of reactants impinging on the sample surface and isothermal reaction conditions. In all of these experiments, a continuous flux of methanol was applied, while atomic oxygen provided by a thermal cracker was pulsed onto the surface employing in all experiments an excess (factor of > 10) of methanol in the gas phase, as compared to the atomic oxygen flux. Time-resolved mass spectrometry was employed to detect the partial oxidation product MeFo in the gas phase, while in-situ IRAS was used to detect adsorbed species, such as formate, an intermediate of the overoxidation reaction. As model catalysts, a flat Au(111)- and a stepped Au(332)-surface were used. As the Au(332)-surface exhibits (111)-terraces with LCS (monoatomic steps) a direct comparison of the two surfaces allows to disentangle the effect of LCS accounting for about 17 % of surface sites on Au(332) and an even larger fraction of surface sites in applied np-Au catalysts. To enhance the microscopic understanding of the surface

processes, these experiments were complemented by theoretical calculations from the group of Prof. Moskaleva.

In the first publication (see paper (I), Chapter 6), the influence of LCS on the selectivity of the partial oxidation of methanol was studied under rather challenging conditions i.e. a rather high flux of activated oxygen and a temperature and a flux of methanol at which the transient methanol concentration on the surface is rather low. Under these conditions, the formation rate of MeFo at the end of the first oxygen pulse is clearly lower (factor of approx. 2.5) on Au(111) as compared to the stepped Au(332) surface demonstrating the beneficial effect of LCS for the formation of MeFo (see Figure 4.1(a)). The higher initial rate on the stepped Au(332) surface is attributed to the higher adsorption energies of desorbing reactants and intermediates, such as methanol or formaldehyde, at step sites, which result in increased transient surface concentrations and, thus, a higher rate of the coupling reaction. Additionally, the preferential adsorption of atomic oxygen at step edges may further enhance the rate of MeFo formation which requires also the presence of activated oxygen.

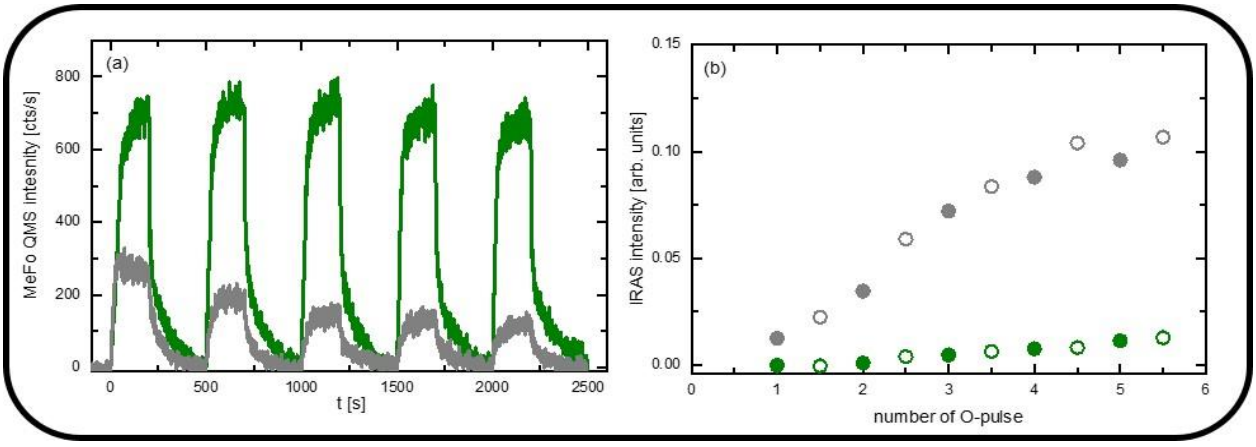

Figure 4.1: Isothermal, pulsed MB measurements on Au(111) (gray) and Au(332) (green) at 230 K with a continuous methanol supply and a pulsed flux of atomic oxygen. (a) MeFo formation rate measured by MS. (b) Formate accumulation given as (integrated) ν_s(OCO)-IRAS-intensity around 1330 cm^{-1}.

Over the course of the pulsed MB experiments, MeFo formation significantly decreases on flat Au(111), but remains relatively stable on stepped Au(332). Under the chosen conditions which are rather oxygen-rich (O-rich), i.e. the excess of methanol in the gas phase is rather low (factor of

approx. 10), formate species, intermediates of the undesired overoxidation pathway to CO_2, may accumulate on the surface, which can poison the surface for MeFo formation.[30, 51] The in-situ IRAS measurements (Figure 4.1(b)) reveal a significantly enhances intensity of bands assigned to adsorbed formate on the flat Au(111) as compared to the Au(332) surface. The increase of the formate bands on the Au(111) surfaces tracks with the decrease in MeFo formation, which is in agreement with surface poisoning by formate. In contrast, the deactivation for MeFo formation is much less severe on the stepped Au(332) surface coinciding with a significantly lower formate accumulation for the stepped surface than on Au(111). This higher formate accumulation on Au(111) could be attributed to a higher formate formation rate as compared to the stepped Au(332) surface, while formate decomposition is comparable on both surfaces. These results clearly show the different reactivity at LCS which improves selectivity for the desired product (MeFo) by enhancing its formation and suppressing the undesired overoxidation pathway. However, the lower overoxidation at LCS was not readily expected, since oxygen is known to adsorb preferentially at low-coordinated steps sites forming chain-like structures. This in turn, leads to a high local oxygen concentration on steps expected to increase overoxidation in case of similar reactivity of the oxygen species. To obtain a better microscopic understanding of the surface processes resulting in this unexpected reactivity, DFT calculations and AIMD simulations were conducted in the group of Prof. Moskaleva. The calculations demonstrated that the reactivity difference of LCS cannot be understood considering only reactions with individual oxygen atoms, as the reaction barriers for formate formation are similarly low for terrace and low-coordinated sites, in contrast to the experimentally observed differences in reactivity between the surfaces. Yet, oxygen atoms in the middle of Au_xO_y-chains at steps were found to exhibit notably different reactivity as compared to individual oxygen atoms and oxygen atoms located at the end of Au_xO_y-chains the former showing an overall higher barrier for formate formation. Thus, formation of extended Au_xO_y-chains, limiting the availability of atomic oxygen and terminal oxygen atoms within Au_xO_y-chains, can explain the lower formate accumulation and thus, overoxidation on the stepped surface. AIMD simulations showed fast formation of extended Au_xO_y-chains coinciding with significant surface restructuring for the stepped surface, while on flat Au(111), the formation of extended Au_xO_y-chains was not observed, in agreement with experimental studies showing the formation of rather irregular Au_xO_y-islands.[68, 96, 97] Consequently, a higher concentration of oxygen as individual atoms or at the edge of Au_xO_y islands is expected for Au(111) suggesting higher formate formation

due to lower barriers as compared to oxygen in extended Au_xO_y-chains at steps, in agreement with the experimental results. Thus, the initially unexpected lower overoxidation rate on the stepped Au surface can be understood, when considering the different reactivity of oxygen species even within accumulated Au_xO_y-phases associated with the low-coordinated step sites.

In conclusion, this isothermal MB experiments combined with theory demonstrates that LCS on gold surfaces play a crucial role in steering the selectivity of methanol oxidation towards MeFo. The insights from this study imply that LCS on np-Au enhance the selectivity for partial oxidation of methanol to MeFo by facilitating the formation of extended Au_xO_y-chains and reducing the overoxidation pathway, and that may also contribute to the understanding of the beneficial effect of ozone activation of np-Au. Moreover, the preferential adsorption of reactants on LCS, enhances their importance under low-coverage conditions, where low collision rates limit reactions. This leads to a shift in selectivity from MeFo to formaldehyde in methanol oxidation on np-Au at the gas-solid interface for short contact times. These findings highlight the crucial role of low-coordinated sites in improving the performance and selectivity of np-Au catalysts, offering valuable insights for optimizing their use in industrial partial oxidation reactions.

The promising results from the first paper have motivated an investigation into a broader range of reaction conditions varying temperature as well as fluxes of methanol and oxygen to determine whether this beneficial effect of LCS is a general trend or limited to specific conditions, as published in JPCC (see paper [II], Chapter 6). For methanol rich conditions (flux ratio MeOH:o-atoms of about 600) both surfaces show a clear maximum in selectivity towards MeFo within the observed temperature window (Figure 4.2(a)). On Au(332) the maximal selectivity is found at higher temperature (230 K) as compared to flat Au(111) (190-210 K), more importantly the Au(332) surface shows higher MeFo selectivity above 200 K for this set of flux conditions. This is attributed to the higher adsorption energy of reactants at steps sites allowing for maintaining higher transient concentrations with increasing temperature which are crucial for the reaction rates as their drop can easily overcompensate the increase of rate constants with temperature. On the other hand, at lower temperatures the absence of LCS is more beneficial for MeFo formation. For a successful coupling reaction, formaldehyde needs to encounter both methoxy and activated oxygen before desorbing. Yet, at low temperatures, high (transient) concentrations on the surface

may create obstacles for these encounters, hindering the coupling reaction which is less effective for the surface with lower adsorption energies where this effect sets in at lower temperature.

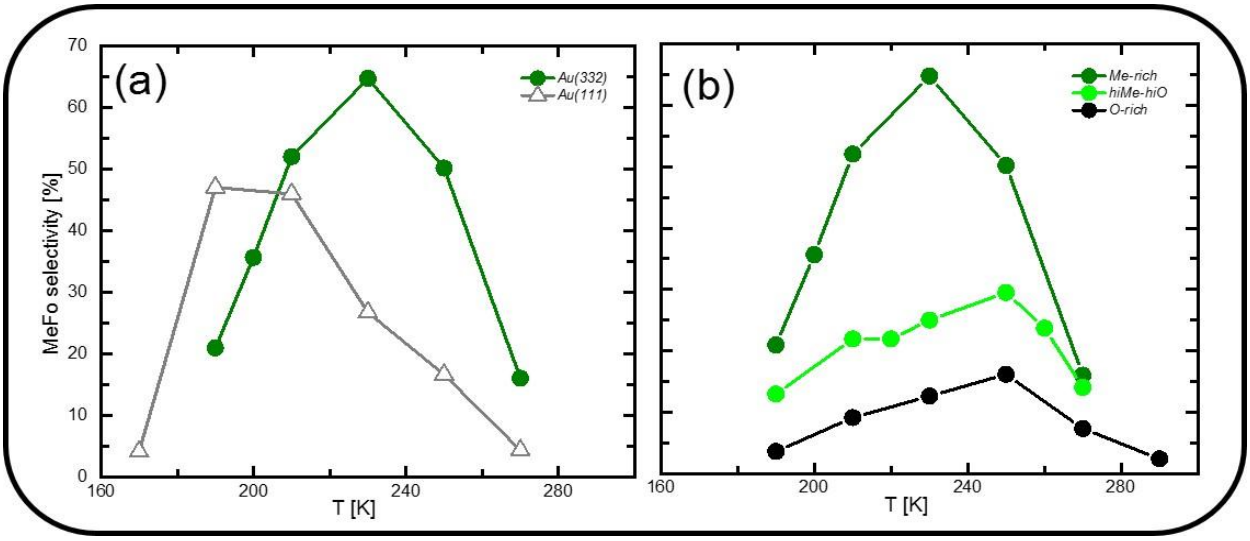

Figure 4.2: (a) MeFo selectivity at the end of the O-pulse in isothermal, pulsed MB experiments on flat Au(111) (open triangles) and stepped Au(332) (filled circles) under Me-rich condition as a function of the surface temperature. (b) MeFo selectivity for different methanol and O-fluxes on Au(332).

While decreasing oxygen to methanol flux ratios lower the selectivity to MeFo (Figure 4.2(b)), in agreement with previous studies, the temperature of maximum MeFo selectivity is shifted to higher temperatures for higher oxygen fluxes. Based on TPD studies from literature, this was attributed to oxygen stabilizing reactants, such as methanol or formaldehyde, on the surface allowing for higher transient concentrations.[49] Considering, that high oxygen fluxes also lower MeFo formation, this rather beneficial effect reflects the complex role of oxygen species in the methanol oxidation on gold surfaces. Transient kinetics provided further insight into the role of oxygen species, as exemplarily shown in Figure 4.3 for Au(111) applying different oxygen fluxes. For low oxygen flux (Figure 4.3 (a)), an induction period is detected, i.e. initially (almost) no MeFo formation is observed. This period becomes shorter upon increasing the oxygen flux demonstrating that individual oxygen atoms in particular at low fluxes are not sufficient for MeFo formation. This result indicates that accumulated Au_xO_y-phases are beneficial for MeFo formation as their formation becomes faster with increasing oxygen flux (and temperature).

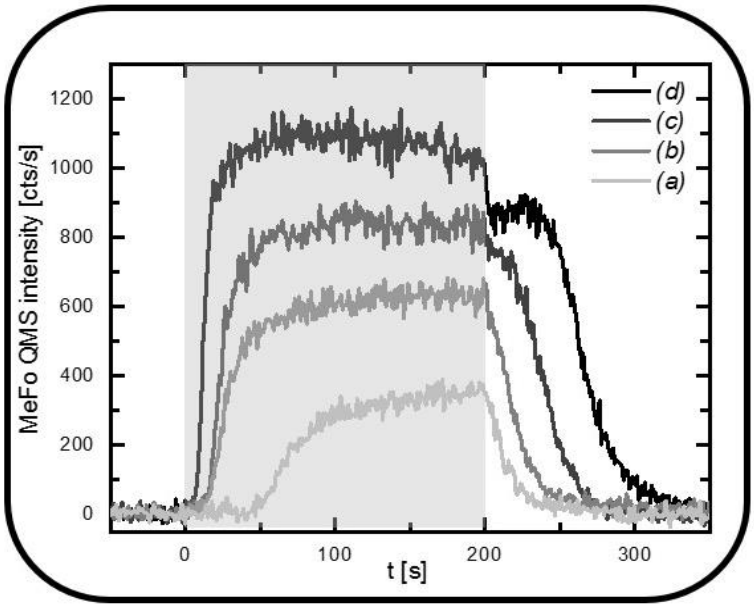

Figure 4.3: Transient MeFo formation kinetics for Au(111) at a low temperature of 190 K for different O-fluxes: (a) $0.04 \cdot 10^{13}$ s^{-1} cm^{-2}, (b) $0.08 \cdot 10^{13}$ s^{-1} cm^{-2}, (c) $0.17 \cdot 10^{13}$ s^{-1} cm^{-2}, (d) $0.4 \cdot 10^{13}$ s^{-1} cm^{-2}. The methanol flux in all experiments was $52.7 \cdot 10^{13}$ s^{-1} cm^{-2}.

While it was previously shown in TPR measurements that the formation of MeFo with accumulated Au_xO_y-phases is feasible,[30] the isothermal MB experiments demonstrated that the accumulation of Au_xO_y species is even necessary for MeFo formation under these conditions. Analysis of the temporal evolution of MeFo formation after the end of the oxygen pulse under higher O-fluxes revealed, moreover, that the accumulated Au_xO_y-phases consist of different oxygen species varying in reactivity which is required to understand the non-monotonic kinetics after the oxygen pulse observed for some reaction conditions. The induction period and the MeFo formation after the end of the oxygen pulse are also observed for the stepped Au(332) surface, but differ significantly from the flat Au(111) surface suggesting a fast and, surprisingly, also a slow process in the formation of Au_xO_y-phases on the stepped surface.[49] AIMD simulations, conducted by the group of Prof. Moskaleva, on the formation of Au_xO_y-phases demonstrated formation of small Au_xO_y-clusters on Au(111) in the presence of Au adatoms (highlighted in orange), as expected after lifting of the herring bone reconstruction of Au(111) (see Figure 4.4(a)).

In the absence of Au adatoms, the root mean square displacements (RMSD) of the Au atoms (blue trace, Figure 4.4(a), right) remained minimal throughout the simulation, no cluster formation is detected highlighting the importance of such low-coordinated surface atoms for formation of accumulated Au_xO_y-phases and accordingly MeFo formation even for flat Au(111). Simulations on a stepped gold surface showed rather fast formation of short Au_xO_y-chains, but a slower formation of extended Au_xO_y-chains which coincides with significant surface restructuring. These

results may not only explain the experimentally suggested fast and slow Au_xO_y formation process on the stepped Au(332) surface, but also imply extended Au_xO_y-chains on restructured steps to especially reactive towards MeFo formation, despite high local oxygen concentrations.

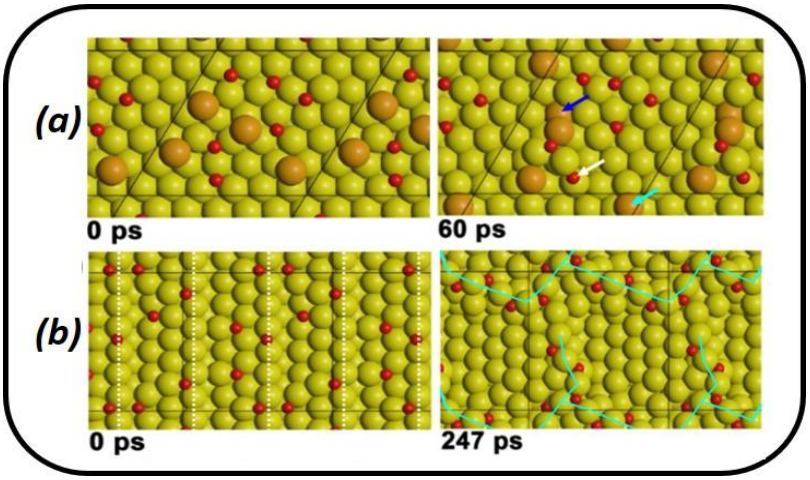

Figure 4.4: Snapshots from AIMD simulations illustrating different degree of surface restructuring induced by adsorbed atomic oxygen (left) and RMSD of the different types of surface atoms (right) on (a) flat Au(111) with Au adatoms and (b) stepped Au(221). Dashed white lines in the initial snapshot (0 ps) indicate the position of the step edges. Color coding: Au, yellow; O, red; Au adatoms (Au(111) surface), orange. These results were obtained by the group of Prof.

In conclusion, this paper extends previous findings by providing a deeper understanding of how surfaces with a high number of low-coordinated sites influence reactivity differently than flat Au(111) surfaces. Specifically, LCS significantly enhance MeFo selectivity at high temperatures, and more generally, under low coverage conditions. Conversely, extended terraces on flat surfaces maintain MeFo selectivity at lower temperatures or higher coverage conditions. Additionally, the experiments provide evidence that MeFo formation benefits from accumulated Au_xO_y-phases or even require their formation under certain conditions. The behavior of these phases varies between different surfaces and can induce significant surface restructuring, especially on stepped surfaces. The results from this paper have significant implications for using np-Au catalysts in aerobic methanol oxidation. Firstly, the combination of extended terraces and LCS in np-Au is crucial for achieving high selectivity towards MeFo. Extended terraces support MeFo formation under high coverage conditions typical of liquid phase reactions, while LCS enhance MeFo selectivity under low coverage conditions in gas phase reactions by preferentially adsorbing reactants and increasing local concentrations. Secondly, the restructuring effect may be a crucial ingredient for further understanding the beneficial role of ozone pre-treatment on np-Au catalysts. This restructuring enhances oxygen activation and catalyst activity, contributing to sustained high MeFo selectivity after an initial

overoxidation phase. This highlights the critical role of different oxygen species in both overoxidation and MeFo formation, challenging the notion of uniformity and structure insensitivity. These findings highlight the need to consider accumulated phases and the restructuring effects their formation induce to better understand and predict surface reactivity in the catalytic processes on np-Au.

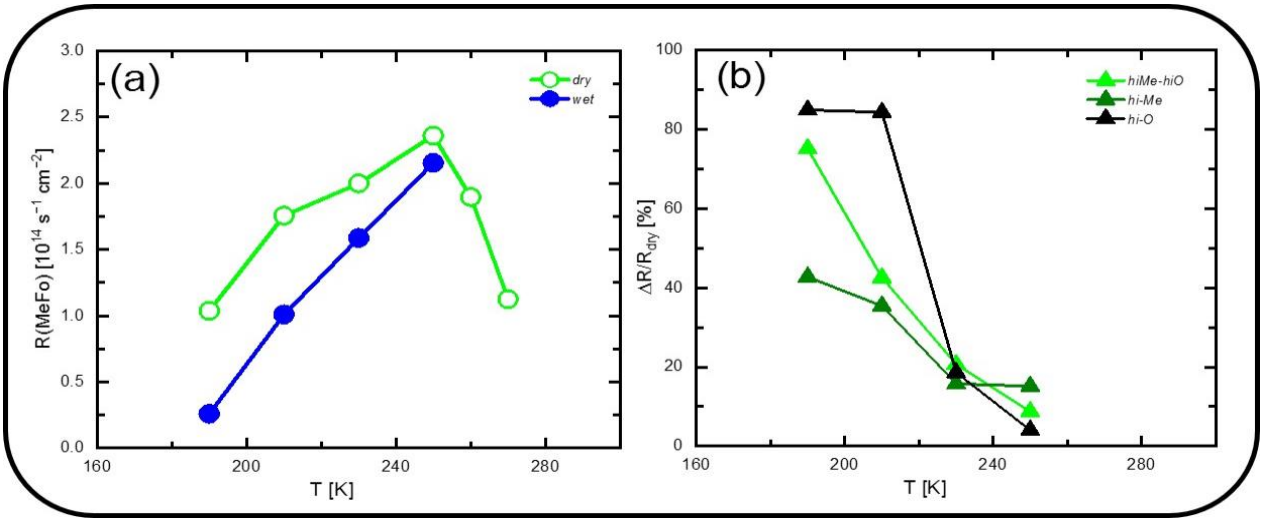

Figure 4.5: (a) MeFo rate in isothermal MB experiments on Au(332) under dry (black) and wet (blue) conditions as a function of sample temperature (b) Relative rate decrease $\Delta R/R_{dry}$ in MeFo formation under wet as compared to dry conditions in isothermal pulsed MB experiments on Au(332) for different surface temperatures as well as different flux conditions. Me-rich (green), O-rich (black) and hiMe-hiO (light green).

In the third publication (submitted to The Journal of Physical Chemistry, see paper (III), Chapter 6), the kinetic importance of water, on the selectivity in methanol oxidation on gold was addressed by pulsed MB experiments in the presence and absence of a high additional flux of water. The latter condition would correspond to methanol conversions of 97 % in the catalyst bed of np-Au assuming 100 % selectivity towards MeFo. The effect of water was investigated in a wide range of reaction conditions, varying temperature as well as fluxes of methanol and oxygen, for both the flat Au(111) surface and the stepped Au(332) surface to clarify the role of LCS also in this respect. Generally, the presence of water lowers the MeFo formation rate as compared to dry conditions, as exemplarily shown in Figure 4.5(a). The negative impact of water decreases with increasing the temperature. This can be expected as an increase of temperature leads to faster water desorption which lowers its transient concentration and therefore, its negative effect on the MeFo formation.

These observations are not limited to this specific set of reaction conditions but are a more general trend of the reaction system (see Figure 4.5(b)). The detrimental effect of water decreases with both lower methanol or oxygen fluxes, thus, for low coverage conditions indicating importantly that interactions of water with both methanol and oxygen (or subsequently formed intermediates) negatively affect MeFo formation.

Water may form hydrogen bonds (H-bond) with methanol or methoxy stabilizing water or affecting the reactivity of the methanol/methoxy lowering thereby the MeFo formation. In-situ IRAS measurements confirmed not only the interaction of methanol/methoxy with water as evidenced by a spectral blue-shift of the C-O stretching mode, but also for specific interactions of water with methanol/methoxy associated with LCS of the Au(332) surface. This agrees with a detailed analysis of the absolute and relative rate decrease in MeFo formation demonstrating that reaction paths for MeFo formation associated with LCS on Au(332) are less affected by water. Presumably this is due to more favorable H-bonding geometries on extended (111)-terraces where methanol was shown to form larger H-bonded structures preferentially along the √3-directions.[49] As this growth direction is not parallel to the steps on Au(332) the corresponding structures cannot be formed on the small (111)-terraces of the Au(332) surface. The presumably less favorable H-bonding geometries minimize the negative impact on MeFo formation at high temperatures where higher binding energies at steps are especially important for maintaining higher transient concentrations and, thus, a high MeFo formation rate.

With oxygen, water may form hydroxyl species (OH) for which theory often predict higher reaction barriers than for oxygen atoms.[42, 92, 93, 98-100] Moreover, water may affect the mobility of oxygen species in accumulated Au_xO_y-phases.[44, 45, 90, 92, 101] The transient MeFo kinetics displaying a prolonged induction period in the presence of water, as exemplarily shown in Figure 4.6 for Au(111) at 190 K, demonstrate the detrimental effect of water on these Au_xO_y-phases for MeFo formation. Under dry conditions a reduction of the oxygen flux by a factor of 2 leads to an induction period of similar length which indicate that water effectively reduces the oxygen species active for MeFo formation by approx. 50 %. The dry and the wet conditions were compared in detail for the conditions at which formate formation was observed in the dry case (see discussion of the second paper above) i.e. the flux of methanol was only about an order of magnitude larger than that of the oxygen atoms.

The effect of water on MeFo selectivity were compared for both surfaces at different temperatures. For Au(111) the deactivation of the surface under wet condition is comparable to that under dry condition. While the deactivation in the dry case correlated with the accumulation of formate that correlation does not hold for the wet case as more formate is accumulated on the surface under these conditions. This suggests, on the one hand, that some of the formate species acts merely as spectator species which do not strongly affect MeFo formation. On the other hand, it indicates a slower formate formation under wet conditions which is consistent with higher activation barriers for reactions with OH compared to oxygen atoms predicted by theory.[42, 92, 93, 98-100] In contrast to that, the Au(332)-surface deactivates strongly in the presence of water under these conditions. While water enhances the accumulation of formate species on Au(332) consistent with a lower selectivity towards MeFo, a more detailed analysis revealed that only a fraction of the formate can impact the reactivity towards MeFo while a significant fraction of formate act as spectator species. Moreover, the increased formate accumulation under wet conditions is inconsistent with the simple picture that the reactions to formate with OH are more activated and thus, slower than with the atomic oxygen, as suggested for flat Au(111). As previously evidence for the importance of Au_xO_y-chains at steps for an overall low formate formation on stepped Au(332) was found (first paper), the increased formate formation in the presence of water could be related to water-induced changes in these Au_xO_y-chains.

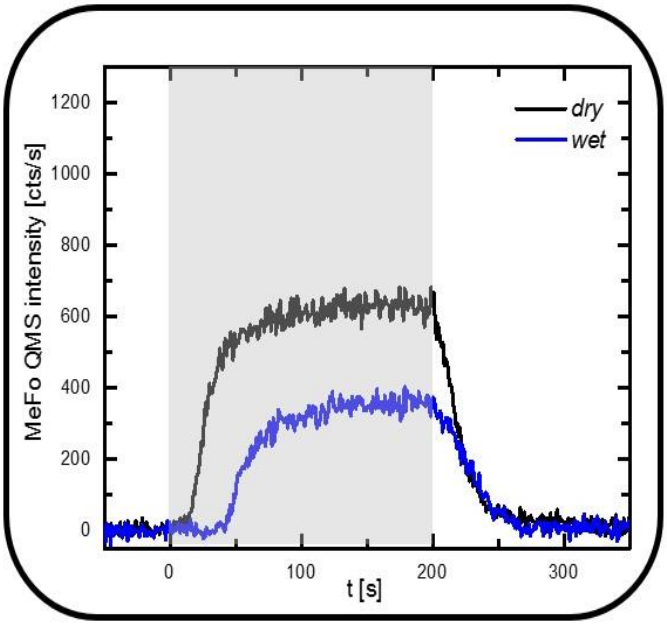

Figure 4.6: Transient MeFo formation rate (m/z = 60) in isothermal pulsed MB experiments of the methanol oxidation under dry (black) and wet (blue) conditions on Au(111) at 190 K.

To obtain further insights into the effect of water on Au_xO_y-chains at steps, theoretical calculations were conducted by the group of Prof. Moskaleva. First, the effect of hydroxylation of Au_xO_y-chains on the activation barriers for formate formation was assessed by DFT calculations, as lower

barriers should result in increased formate accumulation. Upon hydroxylation of Au_xO_y-chains and the presence of isolated OH groups on the wet surface may yield more reactive species for formate formation and open additional reaction pathways competing with MeFo formation and enhancing formate formation via formic acid formation. This is consistent with the experimentally observed increased formate accumulation and decreased selectivity to MeFo on stepped Au(332). Inspired by the AIMD simulations presented in the first two papers, which demonstrated formation of extended Au_xO_y-chains from initially formed short chain coinciding with restructuring of the stepped surface under dry conditions, the impact of water on these processes was addressed. Briefly, the simulations showed that formation of highly mobile hydroxyls in the presence of water affects the formation and the shape of longer Au_xO_y-chains. The hydroxyls are either found as individual hydroxyl species or at the end of the Au_xO_y-chains while hydroxyl groups inside of Au_xO_y-chains were not observed. The terminal hydroxyls of short Au_xO_y-chains were found to dissociate from the chains, in contrast to the dry case for which such process was not observed. While the chains with terminal hydroxyls are not propagated, conversion of the hydroxyl to oxygen allows for further chain growth. The average chain length, important for suppressing overoxidation to formate, will depend on the relative rates of these processes and the surface concentrations of the involved species. Moreover, the restructuring of the stepped gold surface is significantly less pronounced under wet conditions which was associated with efficient MeFo formation on the stepped surface under dry conditions. The theoretical calculation provide, thus, microscopic explanations of the experimental observations on stepped Au(332).

As typically rather oxygen-poor and methanol-rich conditions are expected for applied np-Au catalysts, also MB experiments with an extended pulse sequence were conducted under more methanol-rich conditions. The effect of water on the deactivation for MeFo formation across the pulse sequence is negligible under these conditions for both surfaces. For the stepped Au(332) surface, however, at high temperatures also the MeFo rates are essentially the same under wet and dry conditions, while a clearly negative effect of water on MeFo selectivity is observed for flat Au(111) highlighting the importance of LCS for the corresponding reaction channels.

In conclusion, the adverse effect of water on the desired MeFo formation is rather small, in particular for conditions where formate formation or oxygen accumulation on the surface is low and LCS are available as is typical in gas phase catalysis on np-Au catalysts and aligns well with

the reported high MeFo selectivity at high conversion rates.[20] It is important to note that on flat terraces water decreases the selectivity towards MeFo underscoring the crucial role of LCS to maintain efficient MeFo formation. The effect of water on the selectivity was however found to depend rather strongly on oxygen coverage. At elevated oxygen fluxes water not only reduces selectivity towards the coupling pathway but also promotes the overoxidation channel on stepped surfaces, presumably by formation of highly mobile hydroxyls altering formation and reactivity of long Au_xO_y-chains at steps considered crucial for maintaining high selectivity towards MeFo, as supported by the AIMD simulations. These results shed light on contradictory findings for methanol oxidation on np-Au in gas phase compared to results in liquid phase. In liquid phase catalysis where a high surface concentration has to be expected, water is found detrimental for MeFo selectivity. In gas phase catalysis, however, catalysis is usually done at low-coverage conditions where high selectivity is found for quite large levels of conversion. Based on these results LCS have to be considered crucial for this behavior. Overall, these insights improve the understanding of the role of water in the complex methanol oxidation network on gold catalysts, which provide additional insight which can help a rational improvement of applied np-Au catalysts.

5 Conclusions and outlook

In this work, the methanol oxidation on gold surfaces was investigated under well-defined single collision conditions by isothermal molecular beam (MB) experiments using time-resolved mass spectrometry (QMS) for detection of gas phase products, such as methyl formate (MeFo), and in-situ IRAS measurements for studying surface adsorbates. To elucidate the influence of low-coordinated sites (LCS) on the selectivity, experiments were conducted on a flat Au(111) surface and a stepped Au(332) surface. For unraveling the impact of water, which is a product of the methanol oxidation and also a common (methanol) feed impurity, experiments were conducted in the presence and absence of an added water flux. Theoretical calculation conducted in the group of Prof. Moskaleva were used to enhance the microscopic understanding of surface processes in the investigated systems.

The results show that the steps on Au(332) lower unwanted overoxidation to formate which was attributed to formation of extended Au_xO_y-chains associated with step sites exhibiting higher barriers for the overoxidation reaction as compared to individual oxygen atoms or oxygen at the end of Au_xO_y-chains. As compared to flat Au(111) the stepped Au(332) shows an enhanced selectivity towards the desired product MeFo is observed for at higher temperatures corresponding to low coverage conditions. Under these conditions the higher binding energies at low-coordinated step sites allow to maintain sufficiently high transient concentrations of reactants, such as methanol or formaldehyde required for the multistep reaction path towards MeFo. In contrast, extended terraces exhibit a higher MeFo formation at low temperatures and correspondingly high coverage conditions, as a high number of surface adsorbates may hamper e.g. the reactive encounter of formaldehyde with methoxy and oxygen as required for the coupling reaction favoring thereby competing formaldehyde desorption. Thus, terrace sites may aid in maintaining the MeFo selectivity at high coverage conditions. The results also highlight the complex role of oxygen species in methanol oxidation to MeFo: While increasing the oxygen-to-methanol flux ratio lowers MeFo selectivity, oxygen also may stabilize reactants, such as methanol or formaldehyde, at higher temperatures on the surface increasing their transient surface concentrations and thus, the MeFo formation rate. Furthermore, the transient kinetics of MeFo formation clearly demonstrate that MeFo formation may not only be feasible at, but require accumulated Au_xO_y-phases, whereas the

reaction may not proceed with individual oxygen atoms alone. DFT calculations as well as AIMD simulations provided insight into the formation and the reactivity of such Au_xO_y-phases that help to understand the different reactivities observed on the two surfaces and help to explore the heterogeneous reactivity of the resulting Au_xO_y-phases. In particular, AIMD simulations show that on stepped gold surface extended Au_xO_y-chains were formed which also result in a strong restructuring of the low-coordinated step sites. Surface adatoms often present on Au(111) were also found to be crucial for the formation of distinct Au_xO_y clusters on this surface, further highlighting the importance of low-coordinated sites in the methanol oxidation on gold. Interestingly, the calculations evidence that the reactivity of the oxygen atoms differs significantly within the chain showing that overoxidation pathways a suppressed for oxygen atoms within the chain as compared to the terminal ones as well as to oxygen atoms both on the surface as well as on the terrace. These results suggest that LCS on np-Au enhance selectivity for partial oxidation to MeFo by promoting reactant adsorption and the formation of extended Au_xO_y-chains, which inhibit overoxidation. This effect is consistent with results seen in ethanol oxidation, indicating broad applicability. These findings also shed light on the fact that ozone activation of np-Au was found to enhance the performance with respect to this reaction. The ozone treatment deposits oxygen on the surface some of which is an unselective oxidant and leads to total oxidation at the beginning of the reaction, but it also establishes oxygen coverage at LCS which leads to maintained high MeFo selectivity. These findings are not only relevant for methanol oxidation but could also be applicable to other structure-sensitive reactions involving gold catalysts. It also highlights the importance of surface morphology and reaction conditions in the development of catalytic processes for selective oxidation reactions.

The effect of water on the methanol oxidation on gold was studied under well-defined conditions by isothermal pulse MB experiments with and without added water flux for both flat Au(111) and stepped Au(332) surfaces, to clarify also the role of LCS in this aspect. Water generally has a negative impact on MeFo formation, particularly at high surface concentrations of water, oxygen, and methanol, as e.g. expected in liquid phase oxidation on np-Au. In-situ IRAS evidenced interactions of water with methanol/methoxy which is in line with the formation of H-bonds. In addition, water was found to interact specifically to methanol/methoxy adsorbed at low-coordinated step sites which allows to rationalize that water affects MeFo formation differently on LCS and terrace sites. Water also alters oxygen speciation on Au surfaces, influencing thereby the

selectivity in methanol oxidation. On flat Au(111), water lowers the overoxidation pathway to formate species, presumably due to increased barriers for reactions with hydroxyl as compared to individual oxygen atoms. On stepped Au(332), the impact of water on MeFo production depends quite strongly on the oxygen coverage. At rather oxygen rich conditions MeFo formation decreases considerably in the presence of water an effect that is more severe at lower temperature and can at least partially be understood by the formation of formate species. DFT calculations and AIMD simulations suggested that highly mobile hydroxyls formed in the presence of water not only alter reaction barriers and open additional pathways, but also the formation and shape of Au_xO_y-chains at steps, thereby lifting their beneficial effect of suppressing formate formation under dry conditions and enhancing MeFo formation. Under methanol-rich and low-coverage conditions, the adverse effect of water on MeFo formation is significantly smaller and almost negligible for stepped Au(332) emphasizing the beneficial effect of LCS. These results clarify conflicting findings from studies conducted in liquid versus gas phases on np-Au catalysts. Moreover, the study underscores the critical role of low-coordinated sites in mitigating overoxidation effects under oxygen-rich conditions, highlighting conditions crucial for optimizing np-Au catalysts in achieving high MeFo selectivity.

While this work has enhanced the understanding of oxidation reactions on gold surfaces, a number of questions may merit additional investigations. Even though, the overoxidation of MeFo has been previously investigated on the stepped Au(332) surface suggesting LCS to be important for this reaction,[91] a comparison with a flat Au(111) surface is missing. Transient kinetics reveal valuable information about the reaction network, but the analysis is rather complex if only one of the products can be directly probed. To this end, the addition of intermediates, such as formaldehyde, to the reactant mixture can shed light on the rate-limiting step in methanol oxidation to MeFo. Thus, isothermal pulsed MB experiments, with or without intermediates, can help to unravel their kinetic importance within the reaction network. Moreover, investigating the isothermal reactivity of methanol oxidatively coupled to other alcohols, such as ethanol or cross coupled with amines would be interesting routes to expand on. Initial isothermal pulsed MB experiments with methanol/ethanol mixtures of varying composition show that adding small amounts of ethanol suppresses MeFo formation and other esters, including the self-coupling product of ethanol, ethyl acetate. It is also interesting is to clarify the impact of small amounts of Ag on the methanol oxidation, since it is the residual metal considered crucial for oxygen activation

in the majority of np-Au samples used in catalysis. While residual Ag activates molecular oxygen, it favors methanol overoxidation, unlike Au.[20, 22] Therefore, comparing Ag-containing and Ag-free Au surfaces under isothermal conditions can reveal silver's effect on selectivity towards MeFo and competing reaction products.

Bibliography

(1) Rothenberg, G. *Catalysis: Concepts and Green Applications*, Wiley-VCH, Weinheim, Germany, **2008**.

(2) Farrauto, R. J.; Dorazio, L.; Bartholomew, C. H. *Introduction to Catalysis and Industrial Catalytic Processes*, Wiley, Hoboken, New Jersey, United States, **2016**.

(3) Ali, M. E.; Rahman, M. M.; Sarkar, S. M.; Hamid, S. B. A. Heterogeneous Metal Catalysts for Oxidation Reactions. *Journal of Nanomaterials* **2014**, *2014*, 192038.

(4) Rothenberg, G. *Catalysis*, Elsevier, Amsterdam, Netherlands, **2008**.

(5) Terrasson, V.; Guénin, E. Nanomagnetic-Supported Catalysts. In *Novel Magnetic Nanostructures*, Elsevier, Amsterdam, Netherlands, **2018**.

(6) Woodruff, D. P. *The Chemical Physics of Solid Surfaces, Atomic Clusters: From Gas Phase to Deposited*. Elsevier, Amsterdam, Netherlands, **2007**.

(7) Haruta, M. Size- and Support-Dependency in the Catalysis of Gold. *Catalysis Today* **1997**, *36*, 153-166.

(8) Masatake, H.; Tetsuhiko, K.; Hiroshi, S.; Nobumasa, Y. Novel Gold Catalysts for the Oxidation of Carbon Monoxide at a Temperature far Below 0 °C. *Chemistry Letters* **1987**, *16*, 405-408.

(9) Meyer, R.; Lemire, C.; Shaikhutdinov, S. K.; Freund, H. J. Surface Chemistry of Catalysis by Gold. *Gold Bulletin* **2004**, *37*, 72-124.

(10) Lopez, N.; Janssens, T. V. W.; Clausen, B. S.; Xu, Y.; Mavrikakis, M.; Bligaard, T.; Nørskov, J. K. On the Origin of the Catalytic Activity of Gold Nanoparticles for Low-Temperature CO oxidation. *Journal of Catalysis* **2004**, *223*, 232-235.

(11) Sankar, M.; He, Q.; Engel, R. V.; Sainna, M. A.; Logsdail, A. J.; Roldan, A.; Willock, D. J.; Agarwal, N.; Kiely, C. J.; Hutchings, G. J. Role of the Support in Gold-Containing Nanoparticles as Heterogeneous Catalysts. *Chemical Reviews* **2020**, *120*, 3890-3938.

(12) Lee, J. D.; Miller, J. B.; Shneidman, A. V.; Sun, L.; Weaver, J. F.; Aizenberg, J.; Biener, J.; Boscoboinik, J. A.; Foucher, A. C.; Frenkel, A. I.; et al. Dilute Alloys Based on Au, Ag, or Cu for Efficient Catalysis: From Synthesis to Active Sites. *Chemical reviews* **2022**, *122*, 12600-12650.

(13) Biener, J.; Biener, M. M.; Madix, R. J.; Friend, C. M. Nanoporous Gold: Understanding the Origin of the Reactivity of a 21st Century Catalyst Made by Pre-Columbian Technology. *ACS Catalysis* **2015**, *5*, 6263-6270.

(14) Wittstock, A.; Biener, J.; Bäumer, M. Nanoporous Gold: A New Material for Catalytic and Sensor Applications. *Physical Chemistry Chemical Physics* **2010**, *12*, 12919-12930.

(15) Seker, E.; Reed, M. L.; Begley, M. R. Nanoporous Gold: Fabrication, Characterization, and Applications. *Materials (Basel)* **2009**, *2*, 2188-2215.

(16) Erlebacher, J.; Seshadri, R. Hard Materials with Tunable Porosity. *MRS Bulletin* **2009**, *34*, 561-568.
(17) Ding, Y.; Chen, M. Nanoporous Metals for Catalytic and Optical Applications. *MRS Bulletin* **2009**, *34*, 569-576.
(18) Personick, M. L.; Montemore, M. M.; Kaxiras, E.; Madix, R. J.; Biener, J.; Friend, C. M. Catalyst Design for Enhanced Sustainability Through Fundamental Surface Chemistry. *Philosophical Transactions of the Royal Society A: Mathematical, Physical and Engineering* **2016**, *374*, 20150077.
(19) Zielasek, V.; Jürgens, B.; Schulz, C.; Biener, J.; Biener, M. M.; Hamza, A. V.; Bäumer, M. Gold Catalysts: Nanoporous Gold Foams. *Angewandte Chemie International Edition* **2006**, *45* (48), 8241-8244.
(20) Wittstock, A.; Zielasek, V.; Biener, J.; Friend, C. M.; Bäumer, M. Nanoporous Gold Catalysts for Selective Gas-Phase Oxidative Coupling of Methanol at Low Temperature. *Science (New York, N.Y.)* **2010**, *327*, 319-322.
(21) Xu, C.; Su, J.; Xu, X.; Liu, P.; Zhao, H.; Tian, F.; Ding, Y. Low Temperature CO Oxidation Over Unsupported Nanoporous Gold. *Journal of the American Chemical Society* **2006**, *129*, 42-43.
(22) Xu, B.; Siler, C. G. F.; Madix, R. J.; Friend, C. M. Ag/Au Mixed Sites Promote Oxidative Coupling of Methanol on the Alloy Surface. *Chemistry – A European Journal* **2014**, *20*, 4646-4652.
(23) Francis, S. M.; Leibsle, F. M.; Haq, S.; Xiang, N.; Bowker, M. Methanol Oxidation on Cu(110). *Surface Science* **1994**, *315*, 284-292.
(24) Wachs, I. E.; Madix, R. J. The Oxidation of Methanol on a Silver (110) Vatalyst. *Surface Science* **1978**, *76*, 531-558.
(25) Kaiser, D.; Beckmann, L.; Walter, J.; Bertau, M. Conversion of Green Methanol to Methyl Formate. *Catalysts* **2021**, *11*, 869.
(26) Rong, L.; Xu, Z.; Sun, J.; Guo, G. New Methyl Formate Synthesis Method: Coal to Methyl Formate. *Journal of Energy Chemistry* **2018**, *27*, 238-242.
(27) Christensen, C. H.; Nørskov, J. K. Green Gold Catalysis. *Science* **2010**, *327*, 278-279.
(28) Xu, B. J.; Friend, C. M. Oxidative Coupling of Alcohols on Gold: Insights From Experiments and Theory. *Faraday Discussions* **2011**, *152*, 307-320.
(29) Xu, B.; Madix, R. J.; Friend, C. M. Predicting Gold-Mediated Catalytic Oxidative-Coupling Reactions from Single Crystal Studies. *Accounts of Chemical Research* **2014**, *47*, 761-772.
(30) Xu, B.; Liu, X.; Haubrich, J.; Madix, R. J.; Friend, C. M. Selectivity Control in Gold-Mediated Esterification of Methanol. *Angewandte Chemie International Edition* **2009**, *48*, 4206-4209.
(31) Wang, L. C.; Zhong, Y.; Widmann, D.; Weissmüller, J.; Behm, R. J. On the Role of Residual Ag in Nanoporous Au Catalysts for CO Oxidation: A Combined Microreactor and TAP Reactor Study. *ChemCatChem* **2012**, *4*, 251-259.

(32) Schaefer, A.; Ragazzon, D.; Wittstock, A.; Walle, L. E.; Borg, A.; Bäumer, M.; Sandell, A. Toward Controlled Modification of Nanoporous Gold. A Detailed Surface Science Study on Cleaning and Oxidation. *The Journal of Physical Chemistry C* **2012**, *116*, 4564-4571.

(33) Moskaleva, L. V.; Weiss, T.; Klüner, T.; Bäumer, M. Chemisorbed Oxygen on the Au (321) Surface Alloyed with Silver: A First-Principles Investigation. *The Journal of Physical Chemistry C* **2015**, *119*, 9215-9226.

(34) Moskaleva, L. V.; Röhe, S.; Wittstock, A.; Zielasek, V.; Klüner, T.; Neyman, K. M.; Bäumer, M. Silver Residues As a Possible Key to a Remarkable Oxidative Catalytic Activity of Nanoporous gold. *Physical Chemistry Chemical Physics* **2011**, *13*, 4529-4539.

(35) Wang, L.-C.; Friend, C. M.; Fushimi, R. R.; Madix, R. J. Active Site Densities, Oxygen Activation and Adsorbed Reactive Oxygen in Alcohol Activation on NpAu catalysts. *Faraday discussions* **2016**, *188*, 57-67.

(36) Wang, L.-C.; Zhong, Y.; Jin, H.; Widmann, D.; Weissmüller, J.; Behm, R. J. Catalytic Activity of Nanostructured Au: Scale Effects Versus Bimetallic/Bifunctional Effects in Low-Temperature CO Oxidation on Nanoporous Au. *Beilstein Journal of Nanotechnology* **2013**, *4*, 111-128.

(37) Erlebacher, J.; Aziz, M. J.; Karma, A.; Dimitrov, N.; Sieradzki, K. Evolution of Nanoporosity in Dealloying. *Nature* **2001**, *410*, 450-453.

(38) Zugic, B.; Wang, L.; Heine, C.; Zakharov, D. N.; Lechner, B. A. J.; Stach, E. A.; Biener, J.; Salmeron, M.; Madix, R. J.; Friend, C. M. Dynamic Restructuring Drives Catalytic Activity on Nanoporous Gold-Silver Alloy Catalysts. *Nature materials* **2017**, *16*, 558-564.

(39) Zugic, B.; van Spronsen, M. A.; Heine, C.; Montemore, M. M.; Li, Y.; Zakharov, D. N.; Karakalos, S.; Lechner, B. A. J.; Crumlin, E.; Biener, M. M.; et al. Evolution of Steady-State Material Properties During catalysis: Oxidative Coupling of methanol Over Nanoporous $Ag_{0.03}Au_{0.97}$. *Journal of Catalysis* **2019**, *380*, 366-374.

(40) Wang, L. C.; Personick, M. L.; Karakalos, S.; Fushimi, R.; Friend, C. M.; Madix, R. J. Active Ssites for Methanol Partial Oxidation on Nanoporous Gold Catalysts. *Journal of Catalysis* **2016**, *344*, 778-783.

(41) Liu, X.; Madix, R. J.; Friend, C. M. Unraveling Molecular Transformations on Surfaces: A Critical Comparison of Oxidation Reactions on Coinage Metals. *Chemical Society Reviews* **2008**, *37*, 2243-2261.

(42) Tomaschun, G.; Dononelli, W.; Li, Y.; Bäumer, M.; Klüner, T.; Moskaleva, L. V. Methanol oxidation on the Au(310) surface: A theoretical study. *Journal of Catalysis* **2018**, *364*, 216-227.

(43) Yim, W.-L.; Nowitzki, T.; Necke, M.; Schnars, H.; Nickut, P.; Biener, J.; Biener, M. M.; Zielasek, V.; Al-Shamery, K.; Klüner, T.; Bäumer, M. Universal Phenomena of CO Adsorption on Gold Surfaces with Low-Coordinated Sites. *The Journal of Physical Chemistry C* **2007**, *111* (1), 445-451.

(44) Kim, T. S.; Gong, J.; Ojifinni, R. A.; White, J. M.; Mullins, C. B. Water Activated by Atomic Oxygen on Au(111) to Oxidize CO at Low Temperatures. *Journal of the American Chemical Society* **2006**, *128* (19), 6282-6283.
(45) Jinlong, G.; Ojifinni, R. A.; Kim, T. S.; Stiehl, J. D.; McClure, S. M.; White, J. M.; Mullins, C. B. Low Temperature CO Oxidation On Au(111) and the Role of Adsorbed Water. *Topics in Catalysis* **2007**, *44*, 57-63.
(46) Lackmann, A.; Mahr, C.; Schowalter, M.; Fitzek, L.; Weissmuller, J.; Rosenauer, A.; Wittstock, A. A Comparative Study of Alcohol Oxidation Over Nanoporous Gold in Gas and Liquid phase. *Journal of Catalysis* **2017**, *353*, 99-106.
(47) Stowers, K. J.; Madix, R. J.; Friend, C. M. From Model Studies on Au(111) to Working Conditions With Unsupported Nanoporous Gold catalysts: Oxygen-Assisted Coupling Reactions. *Journal of Catalysis* **2013**, *308*, 131-141.
(48) Senanayake, S. D.; Stacchiola, D. J.; Liu, P.; Mullins, C. B.; Hrbek, J.; Rodriguez, J. A. Interaction of CO with OH on Au(111): HCOO, CO_3, and HOCO as Key Intermediates in the Water-Gas Shift Reaction. *Journal of Physical Chemistry C* **2009**, *113*, 19536-19544.
(49) Gong, J.; Flaherty, D. W.; Ojifinni, R. A.; White, J. M.; Mullins, C. B. Surface Chemistry of Methanol on Clean and Atomic Oxygen Pre-Covered Au(111). *The Journal of Physical Chemistry C* **2008**, *112*, 5501-5509.
(50) Feldt, C. D.; Kirschbaum, T.; Low, J. L.; Riedel, W.; Risse, T. Methanol oxidation on Au(332): Methyl Formate Selectivity and Surface Deactivation Under Isothermal Conditions. *Catalysis Science & Technology* **2022**, *12*, 1418-1428.
(51) Feldt, C. D.; Gimm, T.; Moreira, R.; Riedel, W.; Risse, T. Methanol Oxidation on Au(332): An Isothermal Pulsed Molecular Beam Study. *Physical Chemistry Chemical Physics* **2021**, *23*, 21599-21605.
(52) King, D. A. Thermal Desorption From Metal Surfaces: A Review. *Surface Science* **1975**, *47*, 384-402.
(53) Chernyayeva, T.; Ostapov, A. *Hydrogen In Zirconium*, 'Nuclear Fuel Cycle' Science and Technology Establishment, Kharkov, Ukraine, **2013**.
(54) Rettner, C. T.; Auerbach, D. J.; Tully, J. C.; Kleyn, A. W. Chemical Dynamics at the Gas-Surface Interface. *The Journal of Physical Chemistry* **1996**, *100*, 13021-13033.
(55) Kleyn, A. W. Molecular Beams and Chemical Dynamics at Surfaces. *Chemical Society Reviews* **2003**, *32*, 87-95.
(56) Chorkendorff, I.; Niemantsverdriet, J. W. *Concepts of Modern Catalysis and Kinetics*, Wiley-VCH, Weinheim, Germany, **2003**.

(57) Masel, R. I. *Principles of Adsorption and Reaction On Solid Surfaces*, Wiley, New York, New York, United States, **1996**.
(58) Ibach, H. *Physics of surfaces and interfaces,* Springer, Berlin, Germany, **2006**.
(59) Rettner, C. T.; Auerbach, D. J.; Tully, J. C.; Kleyn, A. W. Chemical Dynamics at the Gas−Surface Interface. *The Journal of Physical Chemistry* **1996**, *100*, 13021-13033.
(60) Benard, J.; Berthier, Y. *Adsorption on metal surfaces : an integrated approach*. Springer, Berlin, Germany, **1983**.
(61) Kleyn, A. W. Molecular Beams and Chemical Dynamics at Surfaces. *Chemical Society Reviews* **2003**, *32*, 87-95.
(62) Polanyi, M.; Wigner, E. Bildung und Zerfall von Molekülen. *Zeitschrift für Physik* **1925**, *33*, 429-434.
(63) Arnaut, L.; Formosinho, S.; Burrows, H. *Chemical Kinetics*, Elsevier , Amsterdam, Netherlands, **2007**.
(64) Feldt, C. D.; Albrecht, P. A.; Eltayeb, S.; Riedel, W.; Risse, T. Heterogeneity of Oxygen Reactivity: Key for Selectivity of Partial Methanol Oxidation on Gold Surfaces. *Chemical Communications* **2022**, *58*, 4336-4339.
(65) Christensen, C. H.; Nørskov, J. K. Green Gold Catalysis. *Science* **2010**, *327*, 278-279.
(66) Wöll, C.; Chiang, S.; Wilson, R. J.; Lippel, P. H. Determination of Atom Positions at Stacking-Fault Dislocations on Au(111) by Scanning Tunneling Microscopy. *Physical Review B* **1989**, *39*, 7988-7991.
(67) Bond, G. C. Relativistic Effects in Coordination, Chemisorption and Catalysis. *Journal of Molecular Catalysis A: Chemical* **2000**, *156*, 1-20.
(68) Min, B. K.; Alemozafar, A. R.; Biener, M. M.; Biener, J.; Friend, C. M. Reaction of Au(111) with Sulfur and Oxygen: Scanning Tunneling Microscopic Study. *Topics in Catalysis* **2005**, *36*, 77-90.
(69) Sander, D.; Linke, U.; Ibach, H. Adsorbate-Induced Surface Stress: Sulfur, Oxygen and Carbon on Ni(100). *Surface Science* **1992**, *272*, 318-325.
(70) Gough, T. E.; Muenter, J. S.; Dymanus, A.; Lainé, D.; Miller, R. E.; Demtröder, W.; Hepburn, J.; Legon, A.; Sloan, J. J.; Valbusa, U. *Atomic and Molecular Beam Methods*, Oxford University Press, Oxford, United Kingdom, **1992**.
(71) Scoles, G. *Atomic and molecular beam methods*, Oxford University Press, New York, NY, **1988**.
(72) Libuda, J.; Freund, H. J. Molecular Beam Experiments on Model Catalysts. *Surface Science Reports* **2005**, *57*, 157-298.
(73) Griffiths, P.; Haseth, J. *Fourier Transform Infrared Spectrometry*. Wiley-Blackwell, Hoboken, New Jersey, **2007**.
(74) Rupprechter, G. Surface Vibrational Spectroscopy on Noble Metal Catalysts From Ultrahigh Vacuum to Atmospheric Pressure. *Annual Reports Section "C" (Physical Chemistry)* **2004**, *100*, 237-311.

(75) Hoffmann, F. M. Infrared Reflection-Absorption Spectroscopy of Adsorbed Molecules. *Surface Science Reports* **1983**, *3*, 107-192.

(76) Francis, S. A.; Ellison, A. H. Infrared Spectra of Monolayers on Metal Mirrors. *Journal of the Optical Society of America* **1959**, *49*, 131-138.

(77) Hollins, P. The Influence of Surface Defects on the Infrared Spectra of Adsorbed Species. *Surface Science Reports* **1992**, *16*, 51-94.

(78) Dawson, P. H. *Quadrupole Mass Spectrometry and Its Applications*. Elsevier, Amsterdam, Netherlands, **1976**.

(79) Urban, P.; Chen, Y.-C.; Wang, Y.-S. *Time-Resolved Mass Spectrometry: From Concept to Applications*, Wiley, Hoboken, New Jersey, United States, **2016**.

(80) Gross, J. H. *Massenspektrometrie: Ein Lehrbuch*, Springer Spektrum, Berlin, Germany, **2013**.

(81) Honour, J. W. Benchtop mass spectrometry in clinical biochemistry. *The Annals of Clinical Biochemistry* **2003**, *40*, 628-638.

(82) Kaklamanos, G.; Aprea, E.; Theodoridis, G. *Chemical Analysis of Food*, Academic Press, San Diego, California, United States. **2020.**

(83) Madey, T. E.; Yates, J. T. Desorption Methods as Probes of Kinetics and Bonding at Surfaces. *Surface Science* **1977**, *63*, 203-231.

(84) Ogura, S.; Fukutani, K. *Compendium of Surface and Interface Analysis*, Springer Singapore, Singapore, **2018**.

(85) Van Hove, M. A.; Weinberg, W. H.; Chan, C.-M. *Low-Energy Electron Diffraction: Experiment, Theory and Surface Structure Determination*, Springer Berlin Heidelberg, Berlin, Germany. **1986**.

(86) McGuirk, G. M. Au(111) Surface Restructuring From Sulfur Adsorbates. Ph.D. Thesis, Pennsylvania State University, Pennsylvania , United States, **2011**.

(87) Deng, X.; Min, B. K.; Guloy, A.; Friend, C. M. Enhancement of O_2 Dissociation on Au(111) by Adsorbed Oxygen: Implications for Oxidation Catalysis. *Journal of the American Chemical Society* **2005**, *127*, 9267-9270.

(88) Liu, X.; Xu, B.; Haubrich, J.; Madix, R. J.; Friend, C. M. Surface-Mediated Self-Coupling of Ethanol on Gold. *Journal of the American Chemical Society* **2009**, *131*, 5757-5759.

(89) Pireaux, J.-J.; Chtaïb, M.; Delrue, J.-P.; Thiry, P.; Liehr, M.; Caudano, R. Electron Spectroscopic Characterization of Oxygen Adsorption on Gold surfaces: I. Substrate Impurity Effects on Molecular Oxygen Adsorption in Ultra High Vacuum. *Surface science* **1984**, *141*, 211-220.

(90) Sault, A. G.; Madix, R. J.; Campbell, C. T. Adsorption of Oxygen and Hydrogen on Au (110)-(1×2). *Surface Science* **1986**, *169*, 347-356.

(91) Feldt, C. D.; Low, J. L.; Albrecht, P. A.; Tang, K.; Riedel, W.; Risse, T. Low-Temperature Oxidation of Methyl Formate on Au(332). *The Journal of Physical Chemistry C* **2021**, *125*, 26522-26529.
(92) Ojifinni, R. A.; Froemming, N. S.; Gong, J.; Pan, M.; Kim, T. S.; White, J. M.; Henkelman, G.; Mullins, C. B. Water-Enhanced Low-Temperature CO Oxidation and Isotope Effects on Atomic Oxygen-Covered Au(111). *Journal of the American Chemical Society* **2008**, *130*, 6801-6812.
(93) Réocreux, R.; Fampiou, I.; Stamatakis, M. The Role of Oxygenated Species in the Catalytic Self-Coupling of MeOH on O Pre-Covered Au(111). *Faraday Discuss* **2021**, *229*, 251-266.
(94) Moreira. Setup of a Molecular Beam Apparatus to study the reactivity of single crystal surfaces and its application to CO oxidation on Au(332). Ph.D. Thesis, Freie Universität Berlin, Berlin, Germany, **2018**.
(95) Libuda, J.; Meusel, I.; Hartmann, J.; Freund, H. J. A Molecular Beam/Surface Spectroscopy Apparatus for The Study of Reactions On Complex Model Catalysts. *Review of Scientific Instruments* **2000**, *71*, 4395-4408.
(96) Min, B. K.; Alemozafar, A. R.; Biener, M. M.; Biener, J.; Friend, C. M. Reaction of Au(111) With Sulfur and Oxygen: Scanning Tunneling Microscopic Study. *Topics in Catalysis* **2005**, *36*, 77-90.
(97) Quiller, R. G.; Baker, T. A.; Deng, X.; Colling, M. E.; Min, B. K.; Friend, C. M. Transient Hydroxyl Formation From Water on Oxygen-Covered Au(111). *The Journal of Chemical Physics* **2008**, *129*, 064-702.
(98) Min, B. K.; Alemozafar, A. R.; Biener, M. M.; Biener, J.; Friend, C. M. Reaction of Au(111) With Sulfur and Oxygen: Scanning Tunneling Microscopic Study. *Topics in Catalysis* **2005**, *36*, 77-90.
(99) Wang, L.; He, C. Z.; Zhang, W. H.; Li, Z. Y.; Yang, J. L. Methanol-Selective Oxidation Pathways on Au Surfaces: A First-Principles Study. *The Journal of Physical Chemistry C* **2014**, *118*, 17511-17520.
(100) Dononelli, W.; Tomaschun, G.; Klüner, T.; Moskaleva, L. V. Understanding Oxygen Activation on Nanoporous Gold. *ACS Catalysis* **2019**, *9*, 5204-5216.
(101) Xu, F.; Fampiou, I.; O'Connor, C. R.; Karakalos, S.; Hiebel, F.; Kaxiras, E.; Madix, R. J.; Friend, C. M. Water facilitates oxygen migration on gold surfaces. *Physical Chemistry Chemical Physics* **2018**, *20*, 2196-2204.

6 Papers

Paper I

Partial oxidation of methanol on gold: How selectivity is steered by low-coordinated sites

Salma Eltayeb, Lenard L. Carroll, Lukas Dippel, Mersad Mostaghimi, Wiebke Riedel, Lyudmila Moskaleva and Thomas Risse, ACS catalysis **2024**, 14, 10, 7901–7906.
DOI: https://doi.org/10.1021/acscatal.3c04578

Contributions

I conducted all experiments and evaluated the experimental data. The theoretical calculations were carried out by group of Prof. Lyudmila Moskaleva. The paper was written by Wiebke Riedel.

Paper II

Selective oxidation of methanol to methyl formate on gold: The role of low-coordinated sites revealed by isothermal pulsed molecular beam experiments and AIMD simulations

Salma Eltayeb, Lenard L. Carroll, Lukas Dippel, Mersad Mostaghimi, Wiebke Riedel, Lyudmila Moskaleva and Thomas Risse, The Journal of Physical Chemistry C **2024**.
DOI: https://doi.org/10.1021/acs.jpcc.4c03959

Contributions

I conducted all experiments and evaluated the experimental data. The theoretical calculations were carried out by group of Prof. Lyudmila Moskaleva. The first draft of paper was written by me.

Paper III

Unraveling the role of water in isothermal methanol partial oxidation to methyl formate on gold: A combined experimental and theoretical study

Salma Eltayeb, Lenard L. Carroll, John Michael Correa Hoyos, Christoph D. Feldt, Benjamin Switon, Wiebke Riedel, Lyudmila Moskaleva and Thomas Risse, submitted to The Journal of Physical Chemistry **2024**.

DOI: https://doi.org/10.1021/acs.jpcc.4c05968

Contributions

I conducted all experiments and evaluated the experimental data. The theoretical calculations were carried out by group of Prof. Lyudmila Moskaleva. The first draft of paper was written by me.